Electron-Cloud Simulations

Giovanni Rumolo & Frank Zimmermann, CERN

(1) e^- cloud build up

– distribution, line & volume density, dose ($\rightarrow$ scrubbing), energy spectrum, heat load, various fields (dipole, solenoids, electrodes,...)

(2) coupled-bunch instability

– bunch-to-bunch wake, growth rate

(3) single-bunch instability

– single-bunch wake, threshold, growth rate, coherent tune shift

(4) incoherent effects

– incoherent tune shift, potential well distortion

(5) synergetic effects: beam-beam, space-charge, impedance

Schematic of simulation recipe

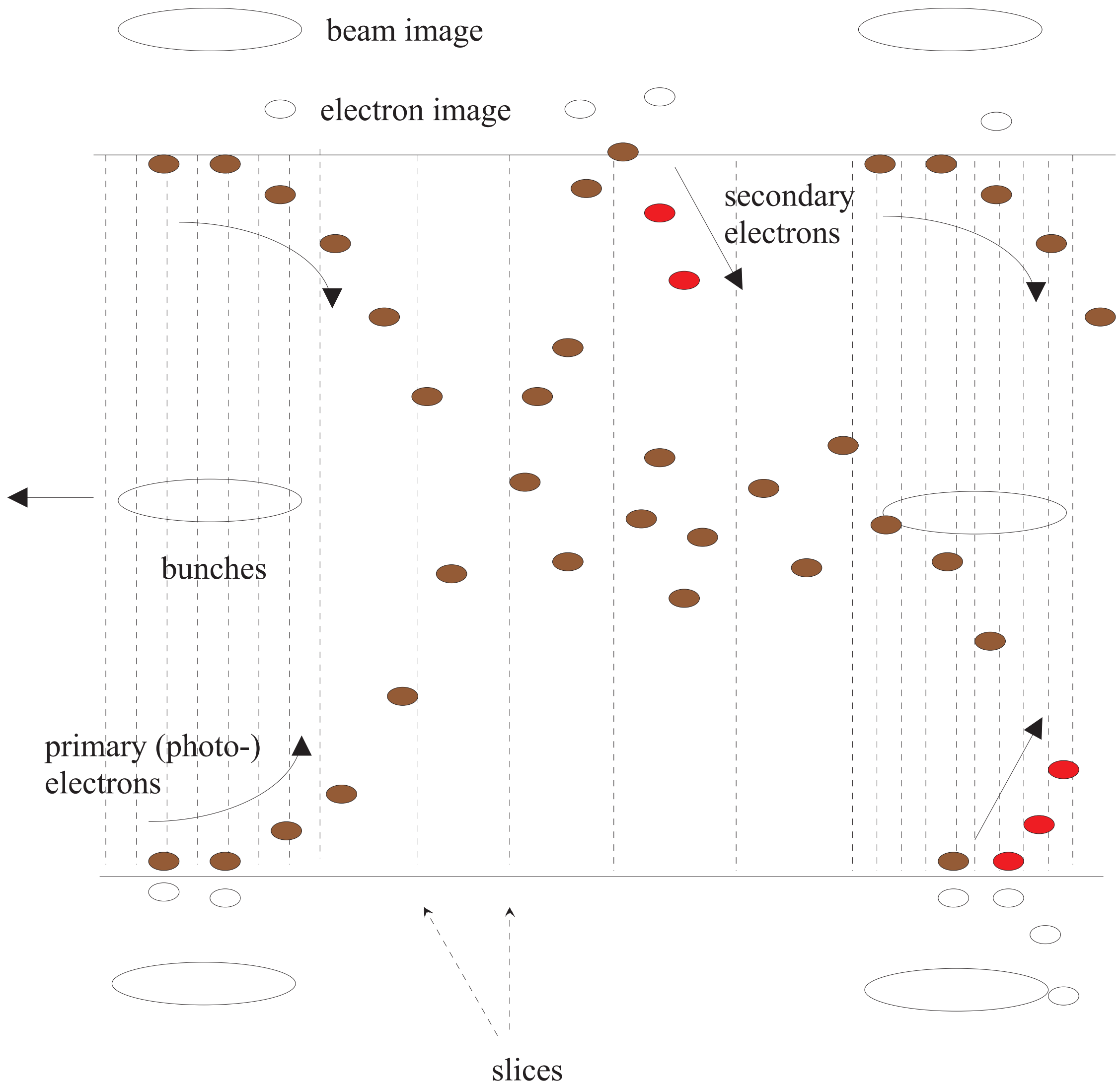

Simulation recipe:

- represent e^- by macro-particles (2000/bunch), split bunches and interbunch gaps into slices
- for each bunch slice, create photoelectrons and accelerate existing e^- in beam and beam-image fields
- if e^- hit the wall $\longrightarrow$ secondary e^-; change macro charge
- at each gap slice the e^- are propagated in the magnetic field; kicks from e^- space-charge and e^- image charges

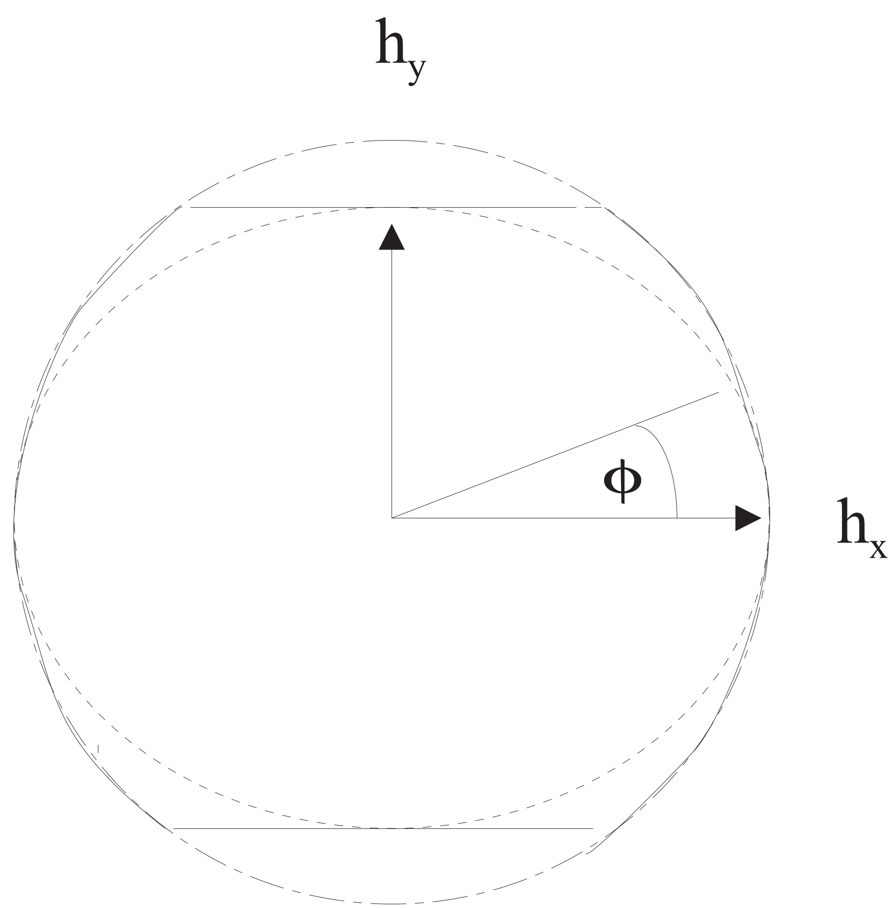

Transverse aperture in the LHC arcs. The solid line describes the actual cross section of the LHC beam screen. Sometimes we approximate it by the inscribed ellipse, *e.g.*, for accurate modeling of image charges.

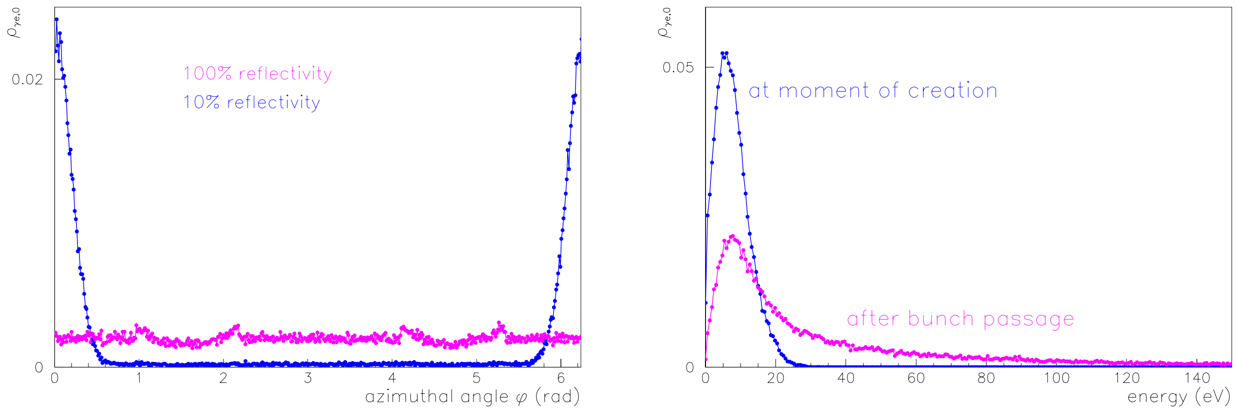

Left: initial azimuthal distribution of photoelectrons for 10% and 100% photon reflectivity; right: initial photoelectron energy distribution at the moment of emission and after the first bunch passage.

CERN

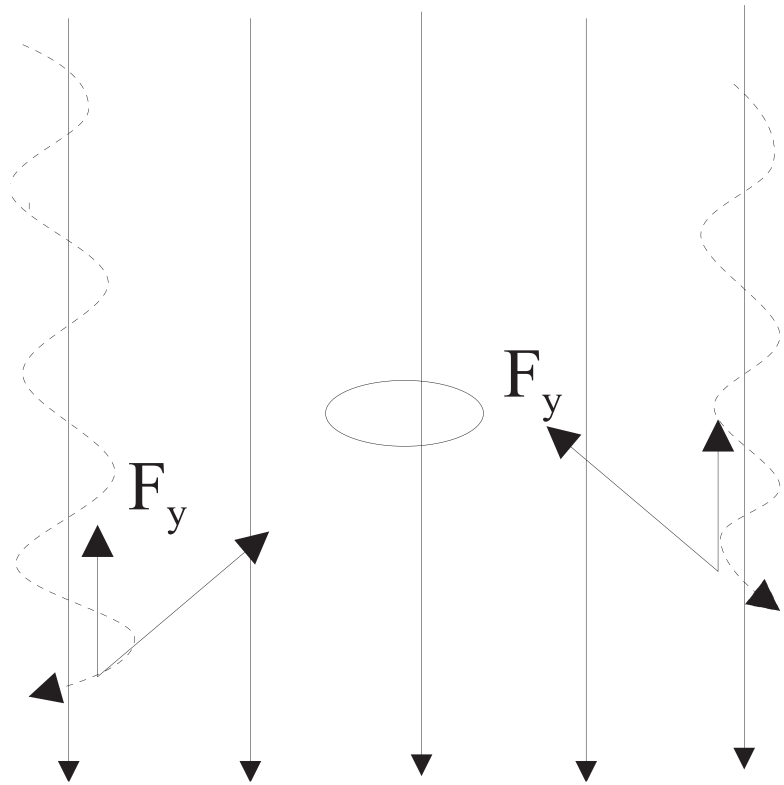

Schematic view of electron motion in a strong vertical dipole field. In the simulation, often only a net vertical kick is applied, since $\frac{eBc}{m_e c^2} \frac{2\sigma_z}{2\pi} \approx 120$ for LHC. Larmor radius 6μm for 200 eV.

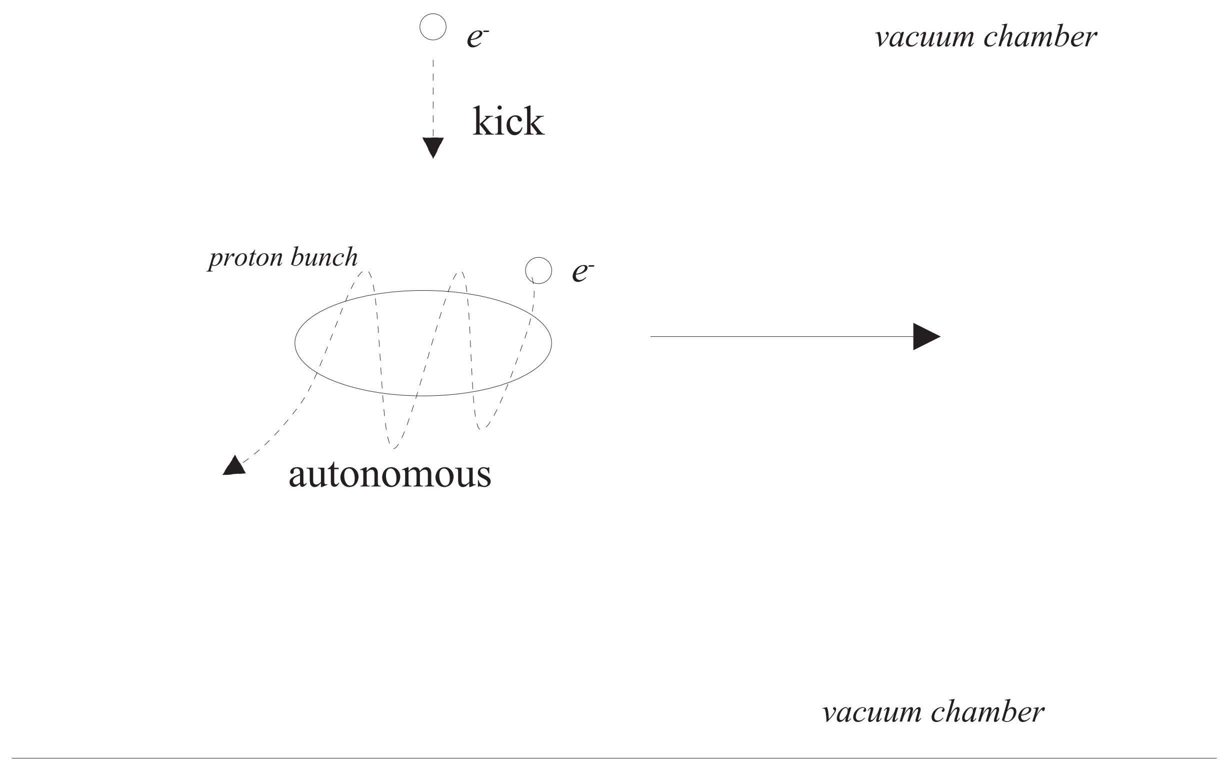

Electrons at large amplitudes do not move much during the bunch passage and simply receive a kick. Electrons near the bunch oscillate in the beam potential. The two situations are called 'kick region' and 'autonomous region', respectively [S. Berg, 1997].

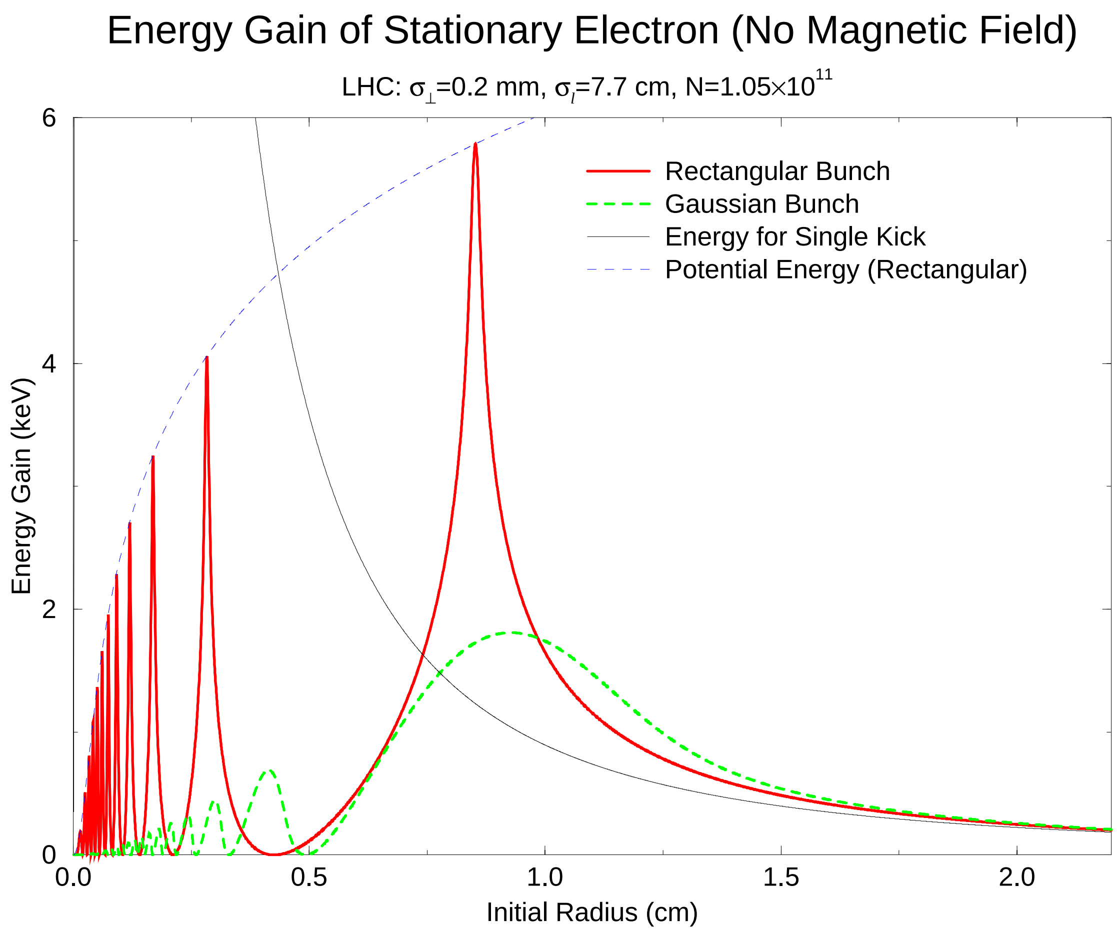

Maximum energy gain vs. initial particle radius for nominal LHC parameters [S. Berg].

CERN

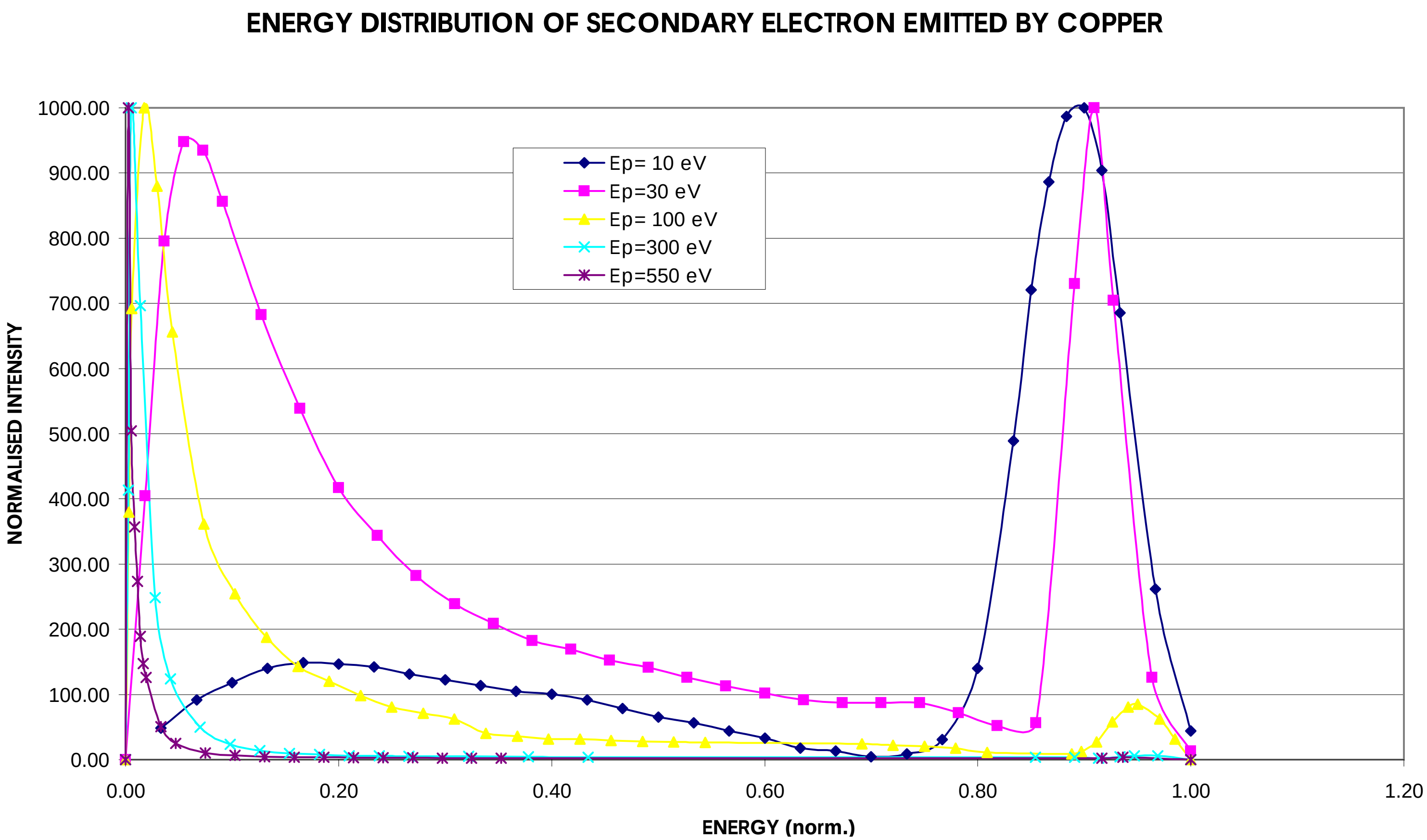

Normalized secondary electron energy distribution for conditioned copper, revealing three components: true secondaries ($E \ll E_p$), elastically scattered ($E \approx E_p$) and rediffused (in between). [N. Hilleret, 2001]

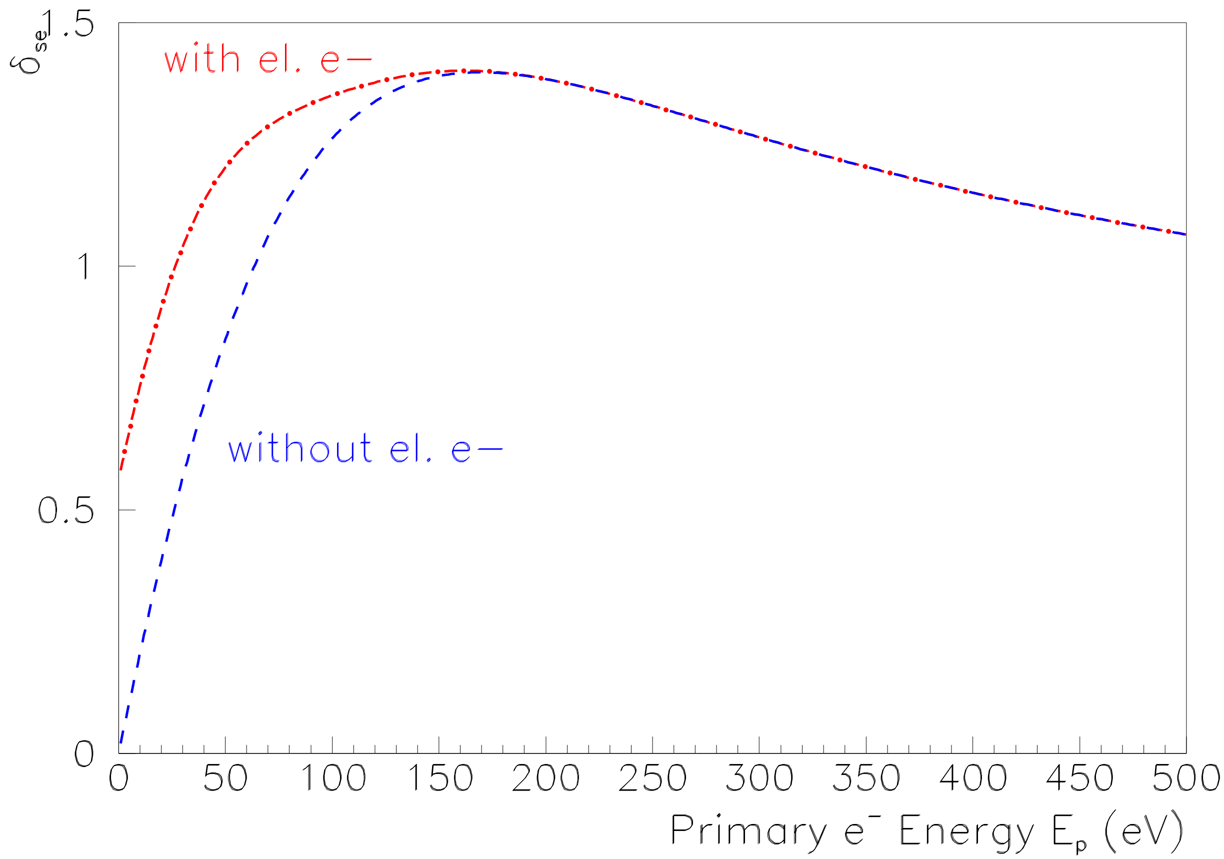

Secondary emission yield for perpendicular incidence vs. primary electron energy with and w/o elastically scattered electrons. Parametrization based on measurements for LHC prototype chamber. [Ian Collins, 2000]

Secondary emission yield: $\delta_{\rm se} = \delta_{\rm tse} + \delta_{\rm el}$

'True secondaries' [Seiler et al.]:

$$\delta_{\rm tse}(E_{\rm p},\theta) = \delta_{\rm max}\, 1.11\, x^{-0.35} \left(1 - e^{-2.3x^{1.35}}\right) \exp\left(0.5\left(1-\cos\theta\right)\right)$$

where θ angle w.r.t. surface normal,
$x = E_{\rm p}\left(1 + 0.7(1-\cos\theta)\right)/\epsilon_{\rm max}$ [Furman, 1997]. Yield for
elast. scattered / rediffused part [Furman, 1997]:

$$\delta_{\rm el}(E_{\rm p}) = \delta_{\rm el,0} + \delta_{{\rm el},E} \exp\left(-\frac{E_{\rm p}^2}{2\sigma_{\rm el}^2}\right).$$

Recent measurements [Ian Collins, 2000]: $\delta_{\rm el,0} \approx 0.0$,
$\delta_{{\rm el},E} = 0.56$, and $\sigma_{\rm el} = 52$ eV.

When e$^-$ hits wall, throw coin:

$\mathrm{rand} < \delta_{\rm el}/\delta\mathrm{se} \;\rightarrow\;$ elastic reflection

Alternative expression for ‘true secondaries’ [M. Furman]:

$$\delta_{\rm tse}(E_{\rm p},\theta) = \delta_{\rm max}\,\frac{s\times x}{s-1+x}\,\exp\left(0.5\left(1-\cos\theta\right)\right)$$

where $s \approx 1.35$ (N. Hilleret), θ angle w.r.t. surface normal, $x = E_{\rm p}\,(1+0.7(1-\cos\theta))/\epsilon_{\rm max}$ [Furman, 1997].

Alternative expression for the yield of elast. scattered / rediffused part :

$$\delta_{\rm el}(E_{\rm p}) = f\delta_{\rm se}(E_{\rm p},\theta)$$

f obtained from measurements

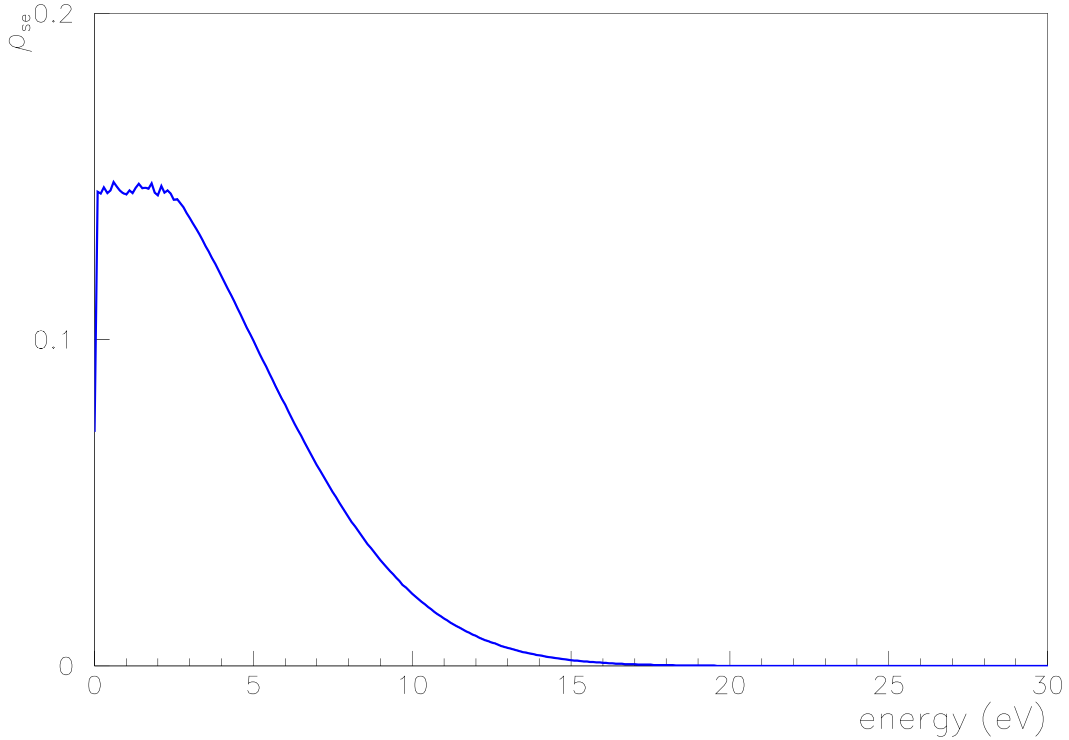

Initial (Gaussian) energy distribution of the true secondary electrons.

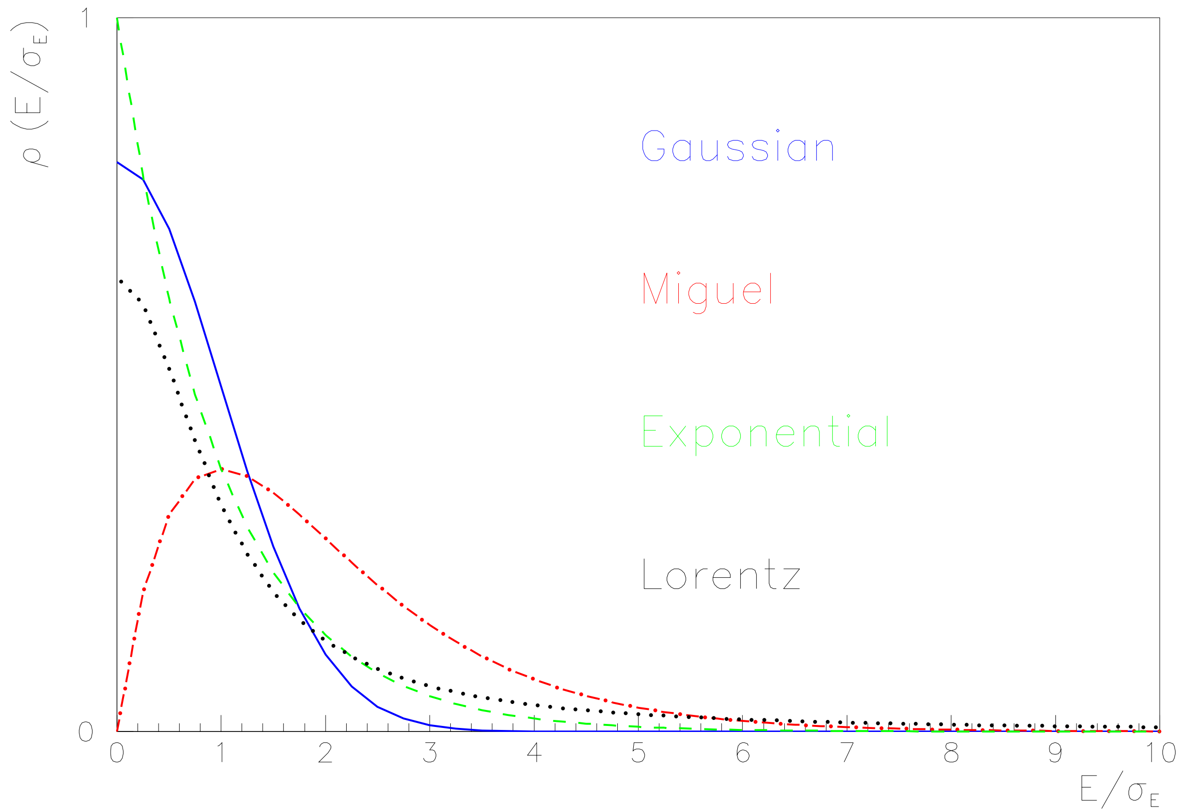

Other energy distributions of true secondaries can be optionally selected.

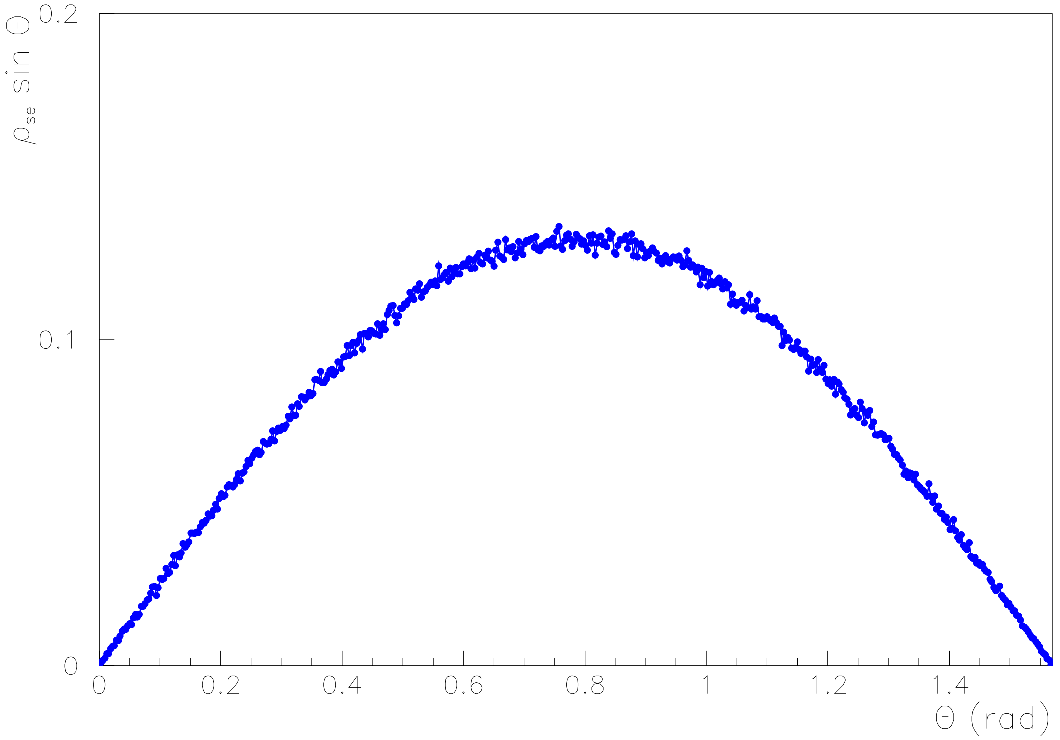

Initial angular distribution $dN/d\theta$ of secondary electrons vs. the polar angle θ w.r.t. surface normal.

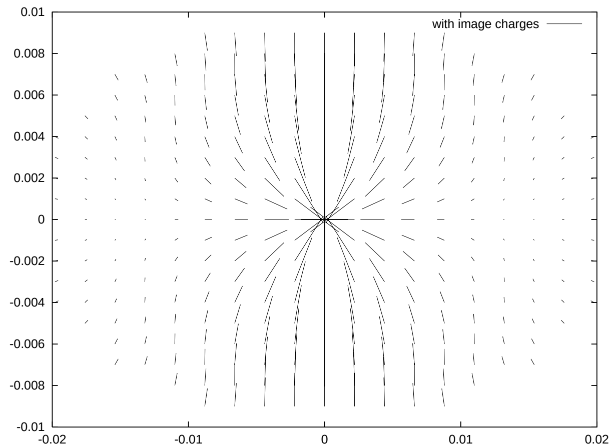

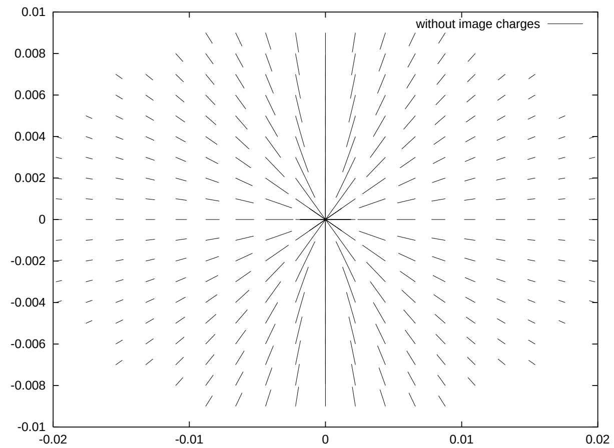

Electric field pattern for a beam centered in an elliptical chamber with [left] and without [right] image charges.

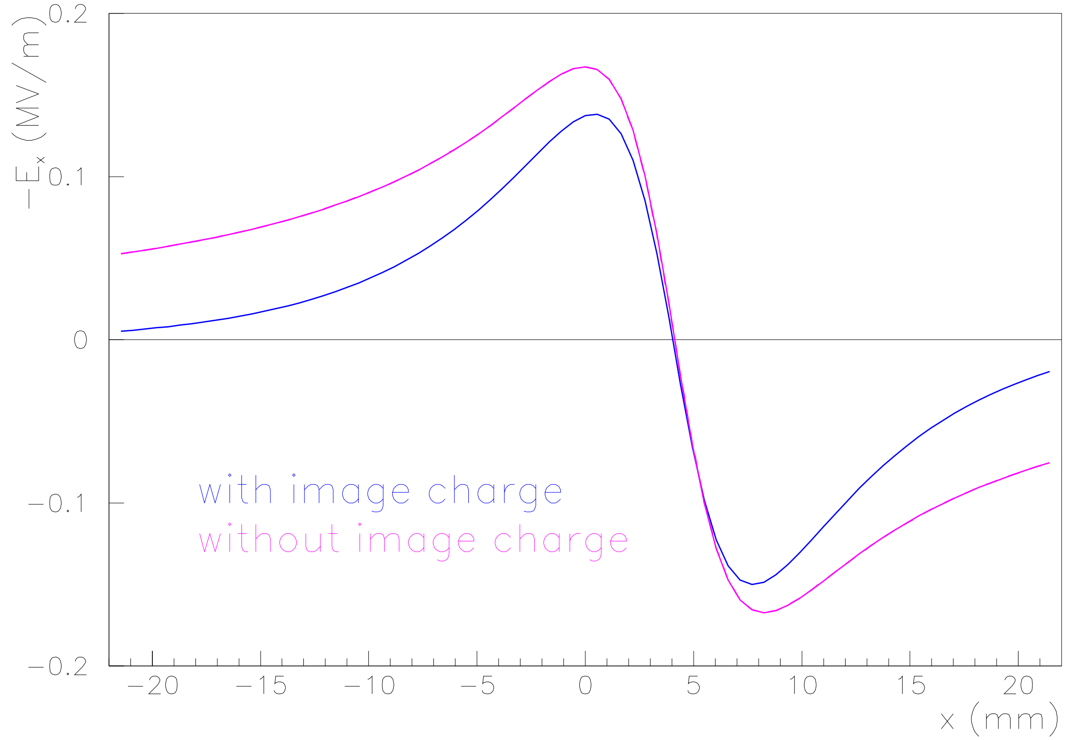

Horizontal electric beam field vs. horizontal position at $y = 0$ for an elliptical chamber with 22×10 mm half apertures and a beam offset of 4.3 mm in both transverse planes.

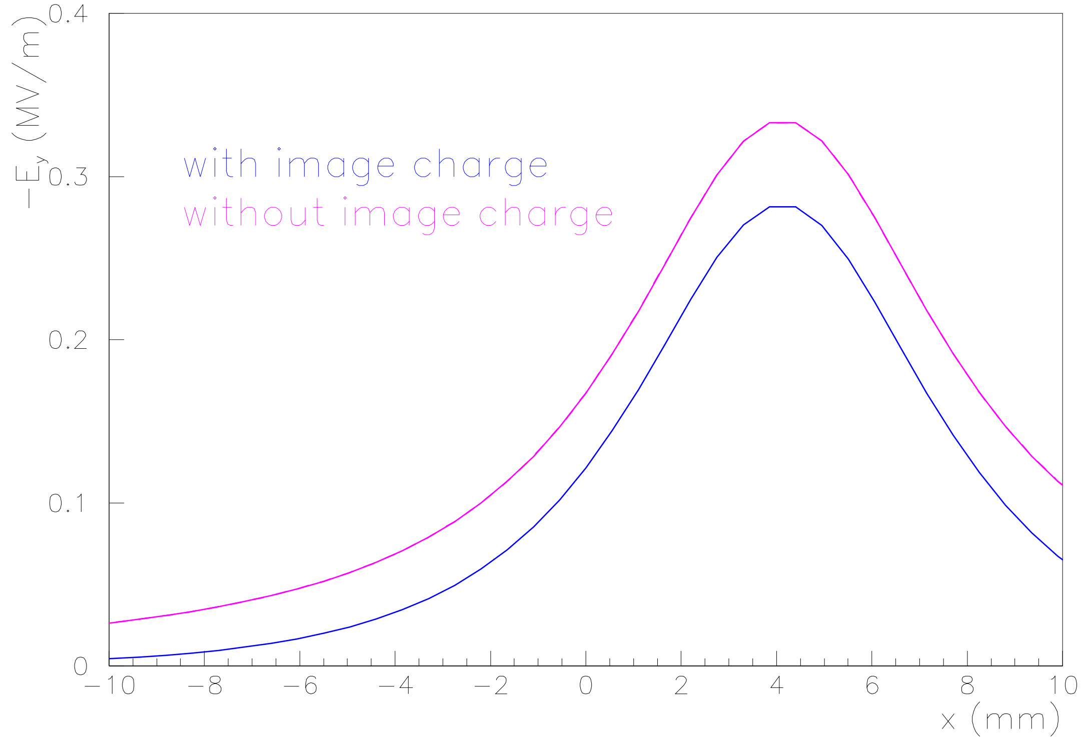

Vertical electric beam field vs. horizontal position at $y = 0$ for an elliptical chamber with 22×10 mm half apertures and a beam offset of 4.3 mm in both transverse planes.

Horizontal electric space-charge field of electron cloud vs. horizontal position after the passage of 8 bunches in the LHC. Parameters: $\delta_{\max} = 2.0$, $Y_{pe} = 0.2$, $R = 0.1$, $\epsilon_{\max} = 300$ eV.

Longitudinal Electron Motion

Contributions: emission angle, beam magnetic field, $\vec{E} \times \vec{B}$ drift in dipole field, typical longit. velocities: 10^5–10^6 m/s.

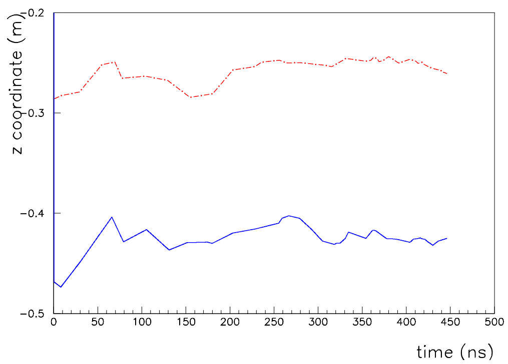

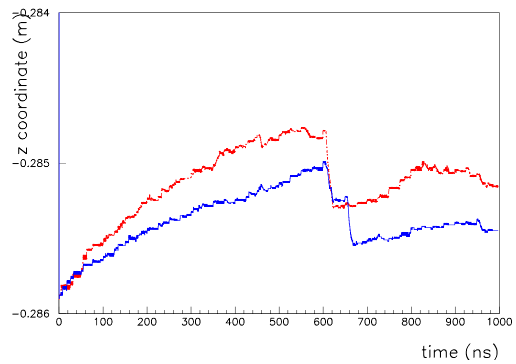

Longitudinal coordinate versus time for two sample electron trajectories in a field free region (left) and in a 1-T dipole field (right). Sometimes neglected.

symbol	LHC (init.)	LHC (fin.)	SPS	PS	KEKB
E [GeV]	7000	7000	26	26	3.5
N_b	10^{11}	10^{11}	10^{11}	10^{11}	3.3×10^{10}
$\sigma_{x,y}$ [mm]	0.3	0.3	3.0, 2.3	2.4, 1.3	0.6–1.0, 0.06–(
σ_z [cm]	7.7	7.7	30	30	0.4
$\beta_{x,y}$ [m]	80	80	40	15	15
$h_{x,y}$ [mm]	22, 18	22, 18	70, 22.5	70, 35	47
$\delta_{\rm max}$	1.9	1.1	1.9	1.9	1.8
$\epsilon_{\rm max}$ [eV]	240	170	300	300	300
R [%]	10	5	100	100	10–100%
$d\lambda_e/ds$ [10^{-6} m^{-1}]	1230	615	0.25	0.05	2000–5000(

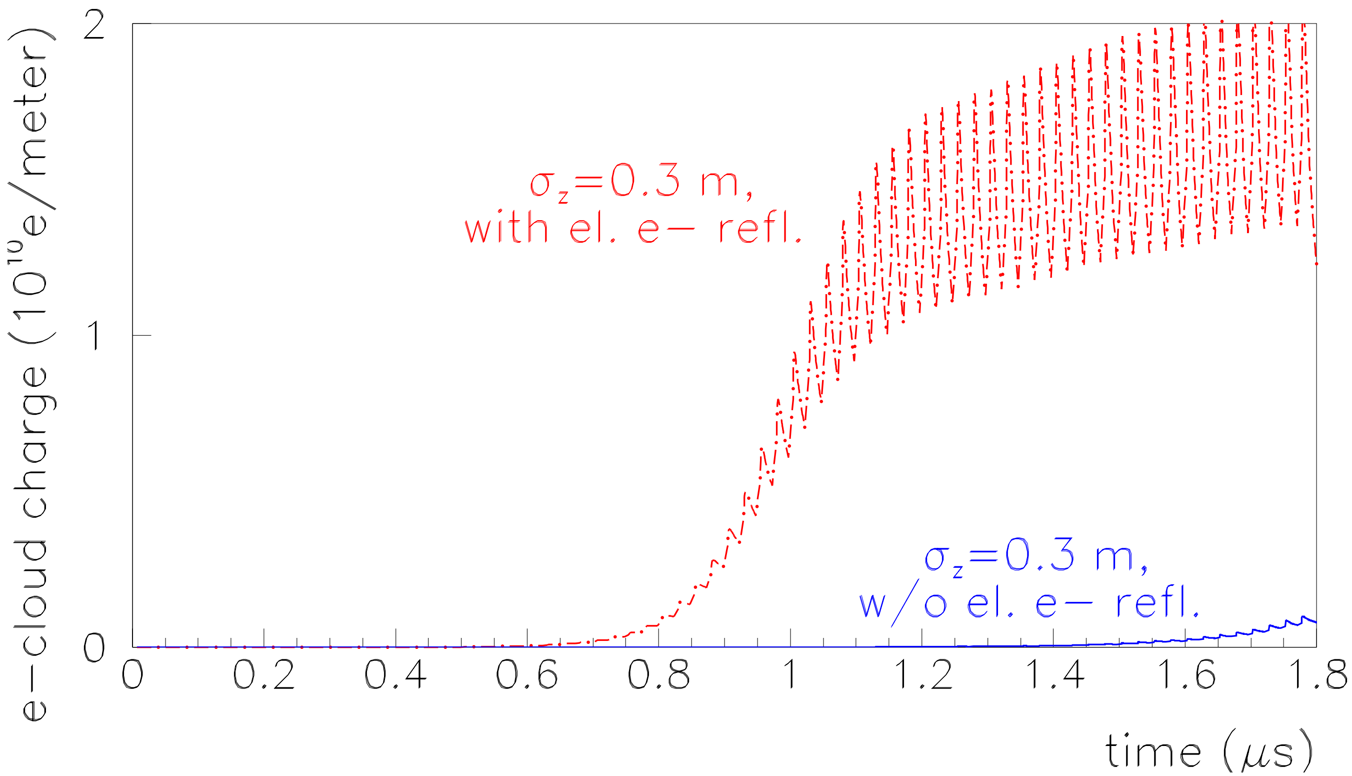

Simulated electron-cloud build up for an SPS dipole chamber, with and without elastic electron reflection. Saturation at $\lambda_{e,\mathrm{sat}} \sim N_b/L_{\mathrm{sep}} \approx 1.3 \times 10^{10}\ \mathrm{m}^{-1} \rightarrow$ 'neutralization' density $\rho_{\mathrm{sat}} \approx N_b/(\pi h_x h_y L_{\mathrm{sep}}) \approx 3 \times 10^{12}\ \mathrm{m}^{-3}$.

$$\Delta Q_{x,y} = h_{y,x}\beta_{x,y} C r_p \rho_e/(\gamma(h_x + h_y)) \approx 0.01 - 0.04$$

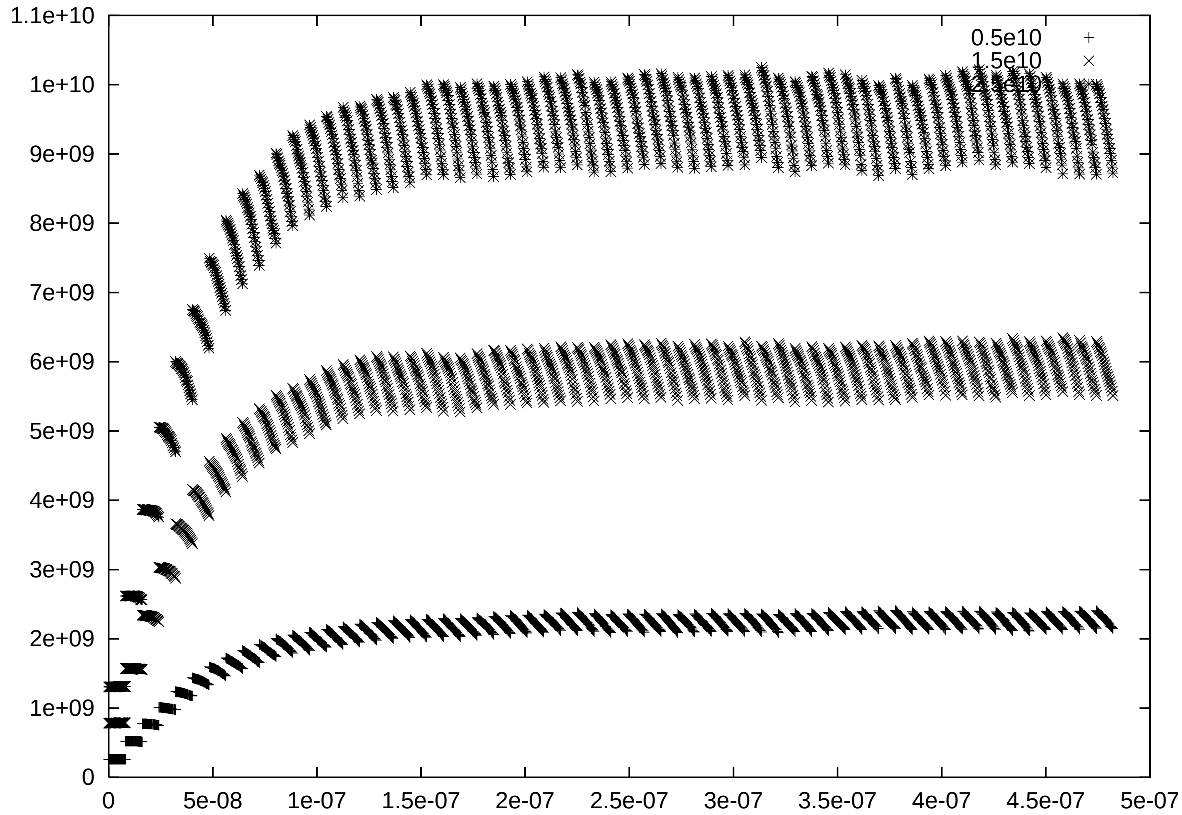

e^- cloud build up (total charge per meter) vs. time (s) in a field-free region of the KEKB LER for $N_b = 5 \times 10^9$, 1.5×10^{10}, 2.5×10^{10}), 4-bucket spacing, $Y = 0.05$/e$^+$/m.

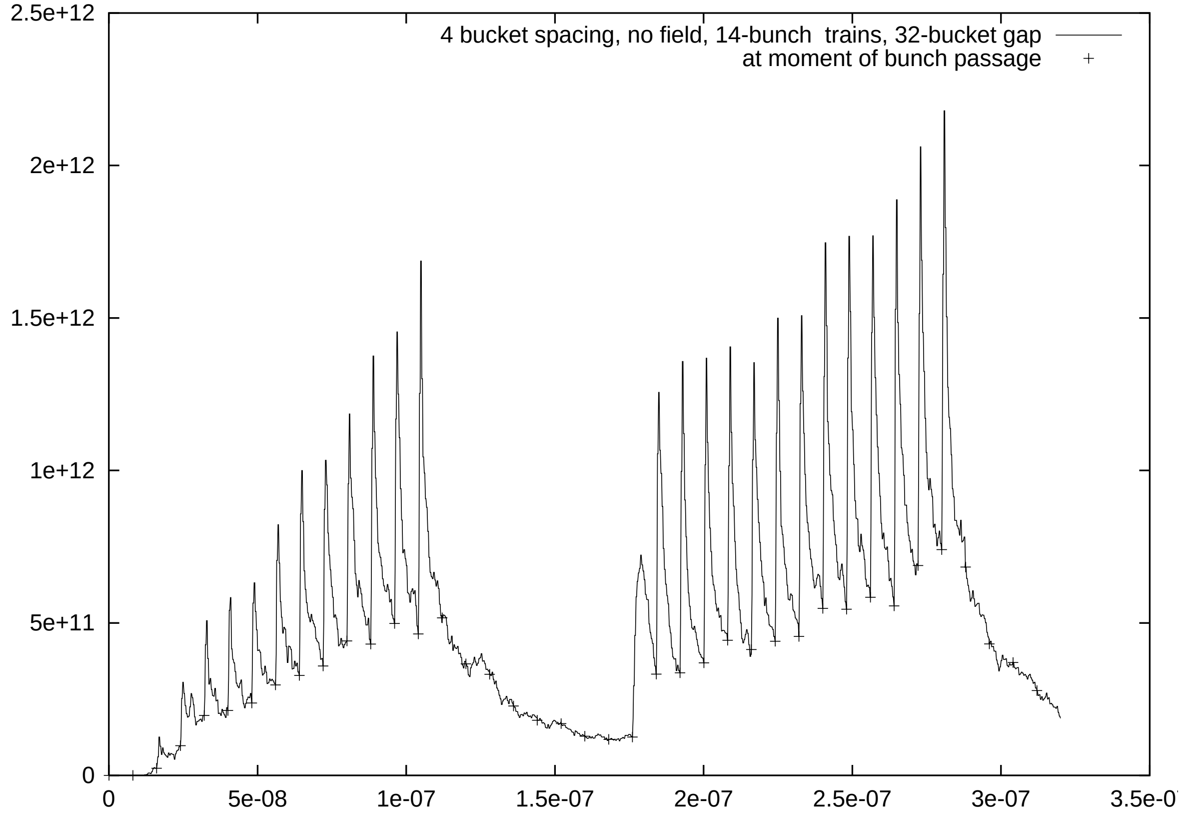

e^- cloud density [m^{-3}] (total charge per meter) vs. time (s) in a field-free region of the KEKB LER for $N_b = 3.3 \times 10^{10}$, 4-bucket spacing, $Y = 0.005$/e$^+$/m and $R = 100\%$.

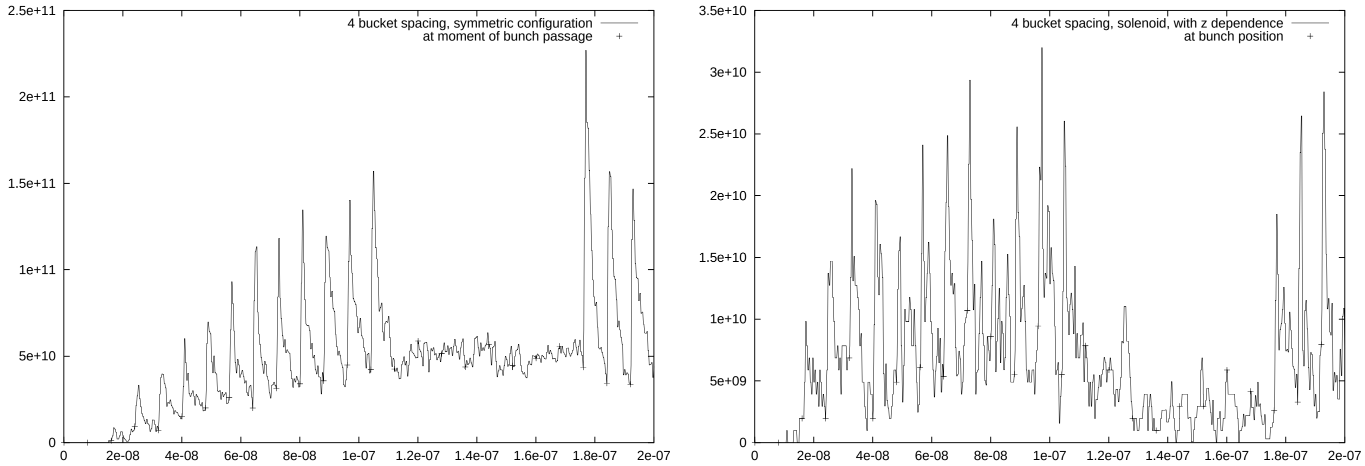

e^- cloud density [m^{-3}] (total charge per meter) vs. time (s) in a perodic quadrupole configuration, with peak gradient of 0.5 T/m, minimum 0.1 T/m and period 10 cm (left) and in a sinusoidal solenoid field with a peak field of ± 50G and 1-m longitudinal period (right), of the KEKB LER for $N_b = 3.3 \times 10^{10}$, 4-bucket spacing, $Y = 0.005$/e$^+$/m and $R = 100\%$.

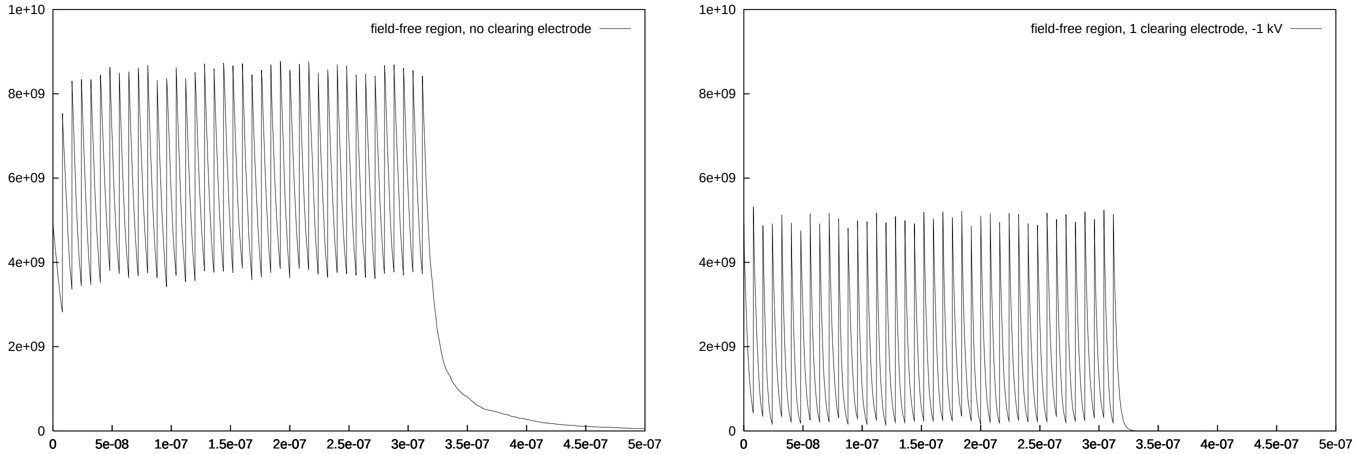

e^- line density in units of m^{-1} in a 1-m long magnetic field-free region of KEKB vs. time in seconds, during and after the passage of a 40-bunch train without clearing electrodes (left), and with a single clearing electrode near the top of the chamber at approximately -1 kV (right).

variable	symbol	CLIC	NLC
beam energy	E	3.5 GeV	1.98 GeV
bunch population	N_b	4.2×10^9	1.5×10^{10}
rms bunch length	σ_z	5 mm	3.6 mm
rms transv. beam size	$\sigma_{x,y}$	18, 1.5 μm	41.5, 9.0 μm
average beta function	β_y	5 m	5 m
norm. hor. emittance	$\gamma\epsilon_x$	4.5×10^{-7} m	3×10^{-6} m
norm. vert. emittance	$\gamma\epsilon_y$	3×10^{-9} m	3×10^{-8} m
bunch spacing	$L_{\rm sep}$	0.2 m	0.84 m
chamber radius	$h_{x,y}$	5 mm	16 mm
primary electron rate in wiggler	$d\lambda_e/ds$	0.075 /e^+/m	
primary electron rate in arc	$d\lambda_e/ds$	0.0025 /e^+/m	6.1 /e^+/m
photon reflectivity	R	10%	10%–100%
maximum secondary emission yield	$\delta_{\rm max}$	1.1–1.7	2.75
probability of elast. reflection for $E_{\rm p} \approx 0$	$\delta_{{\rm el},E}$	0.56	0

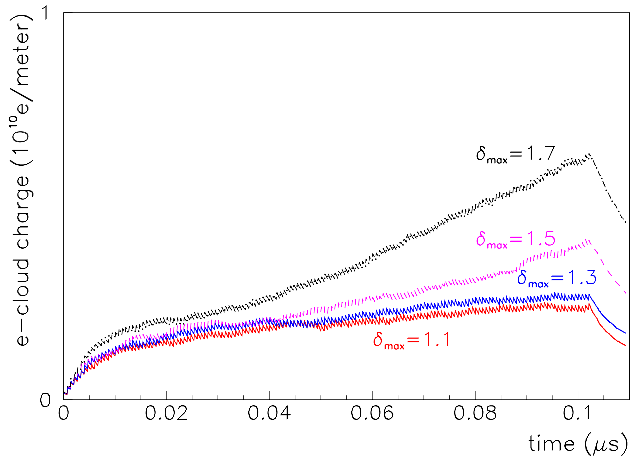

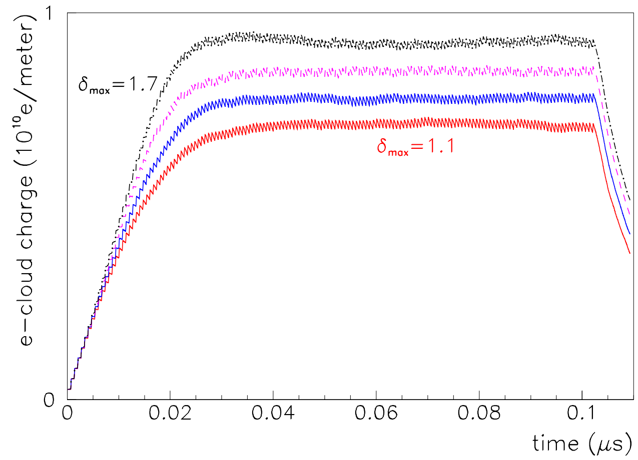

Electron line density in units of 10^{10} m^{-1} vs. time in μs, for the periodic wiggler in CLIC DR (left) and the field-free region behind wiggler (right).

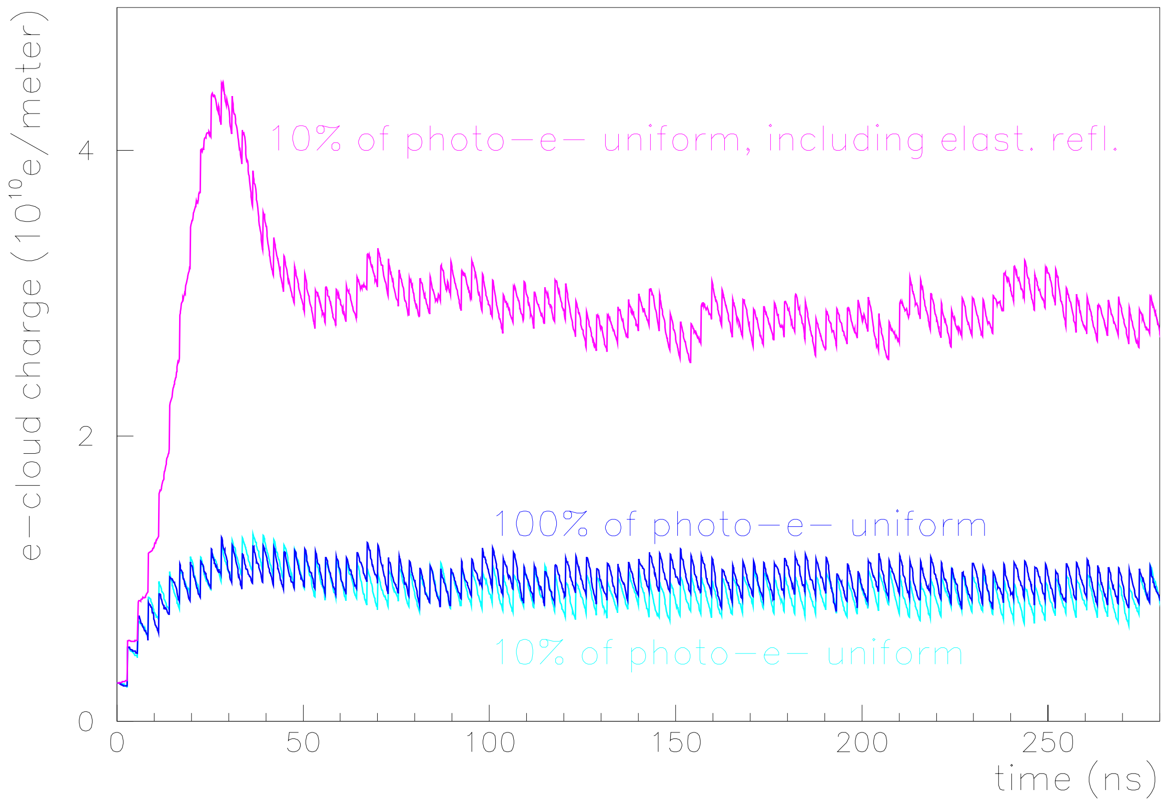

Central electron density in units of m^{-3} for a bellows section in the NLC damping ring. (Parameters courtesy of M. Pivi)

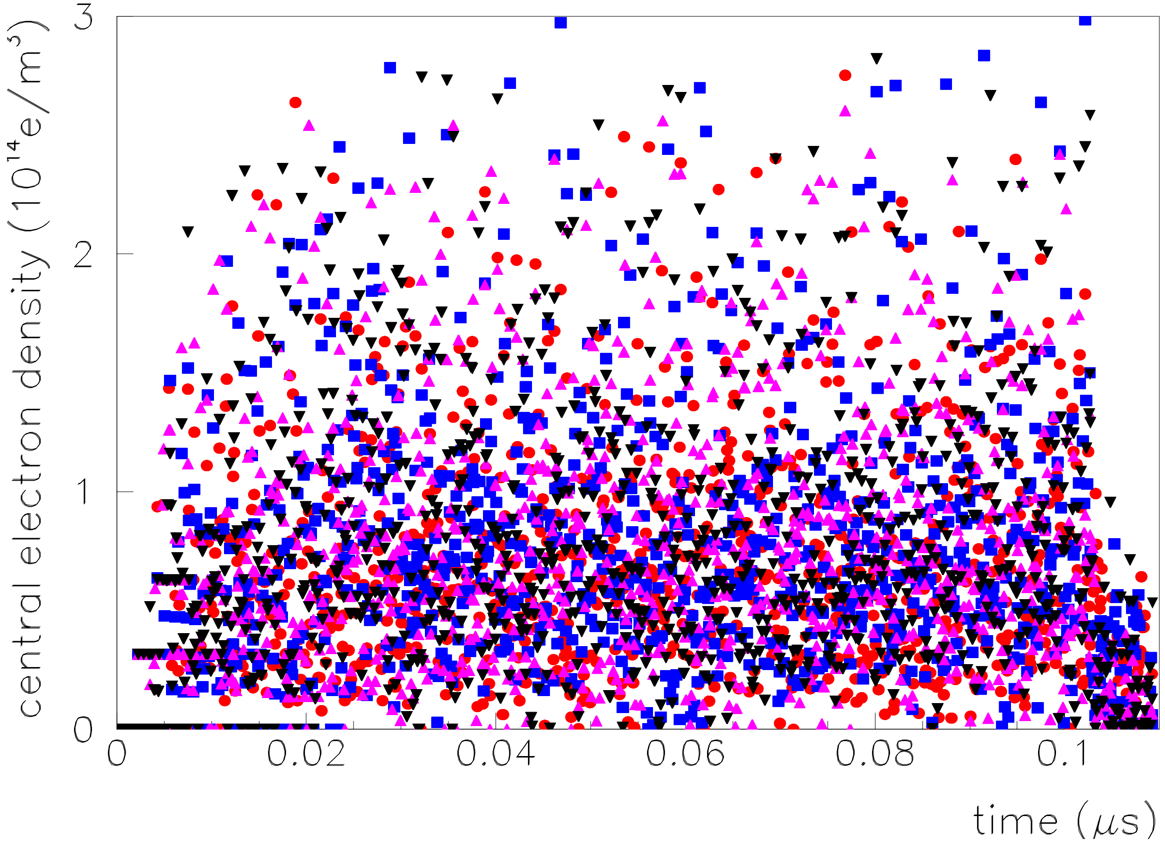

Evolution of central electron density in units of 10^{14} m^{-3} vs. time in μs, for a field-free region behind the CLIC wiggler.

Electrons Incident on the Wall: 'Scrubbing'

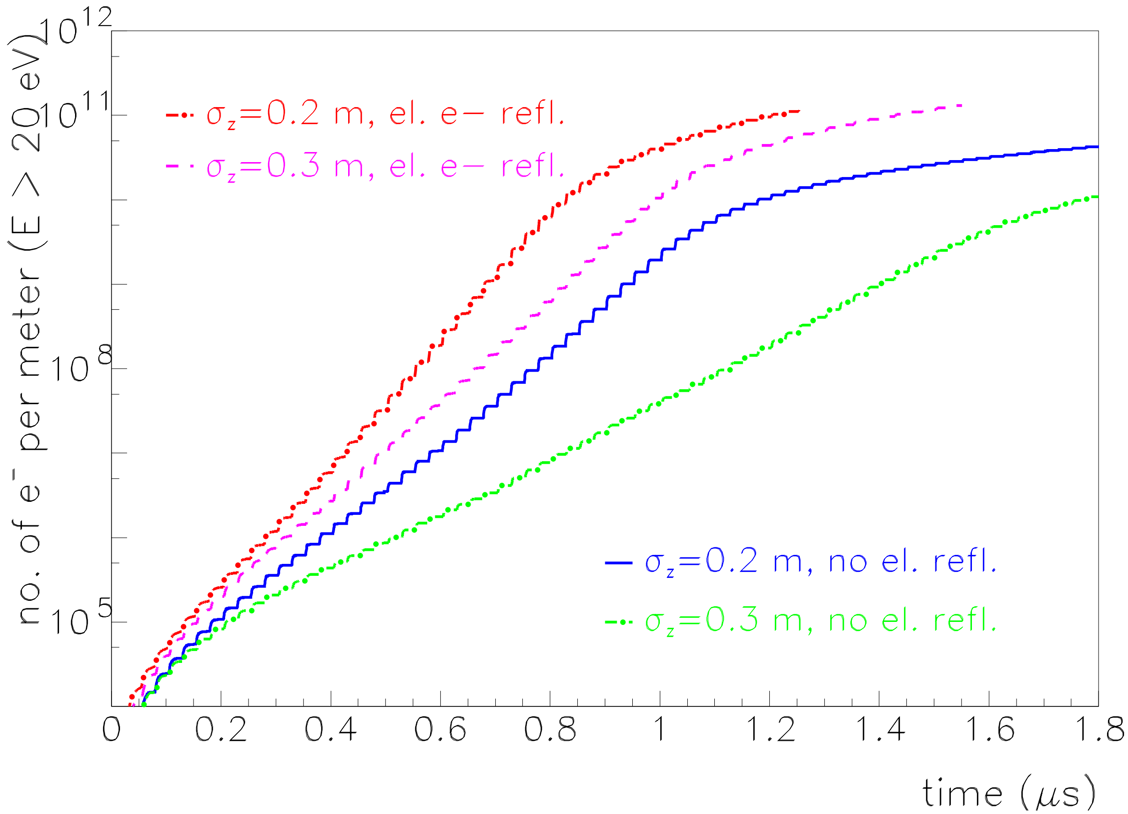

Simulated no. of e^- per meter with $E > 20$ eV hitting the chamber wall during the passage of the 81-bunch LHC batch through an SPS dipole chamber, for $N_b = 4.3 \times 10^{10}$ (May 2000 parameters).

Energy Spectrum of Lost Electron

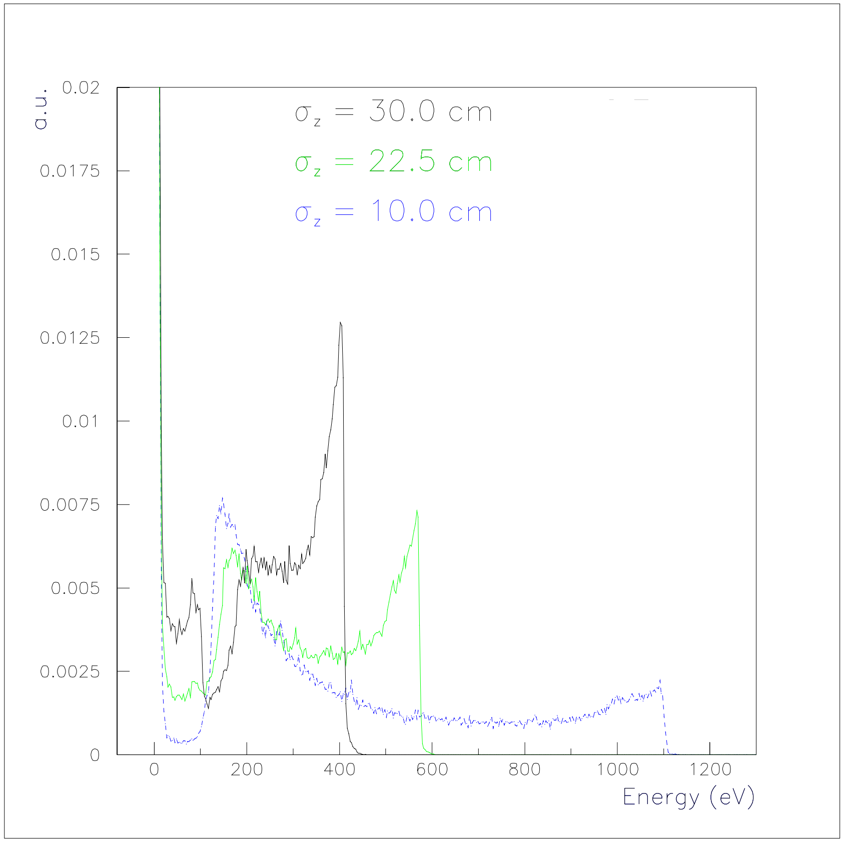

Simulated electron-cloud energy spectrum for different bunch lengths in a field-free region of the SPS [A. Arauzo, F.Z., 2000].

Angular Spectrum of Lost Electron

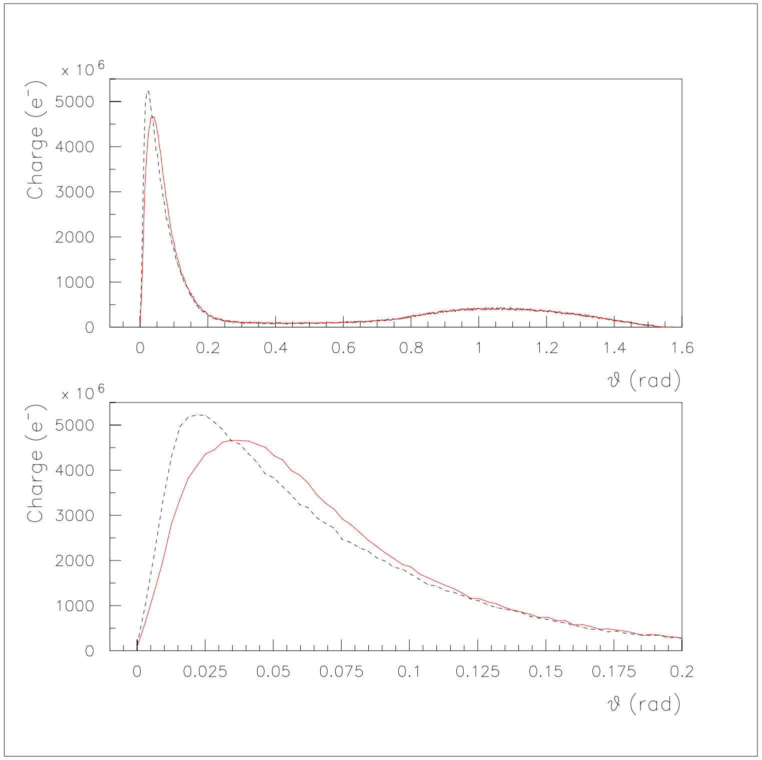

$$\Delta p_{e,x}^{(em)} = \Delta p_{e,x}^{(e)} \left(1 - \frac{v_{e,z}}{c}\right)$$

$$\Delta p_{e,y}^{(em)} = \Delta p_{e,y}^{(e)} \left(1 - \frac{v_{e,z}}{c}\right)$$

$$\Delta p_{e,z}^{(em)} = \frac{v_{e,x}}{c} \Delta p_{e,x}^{(e)} + \frac{v_{e,y}}{c} \Delta$$

Angular distribution of e^- hitting the LHC beam pipe. Red line: with beam magnetic field. Black line: w/o it [A. Arauzo, F.Z., 2000].

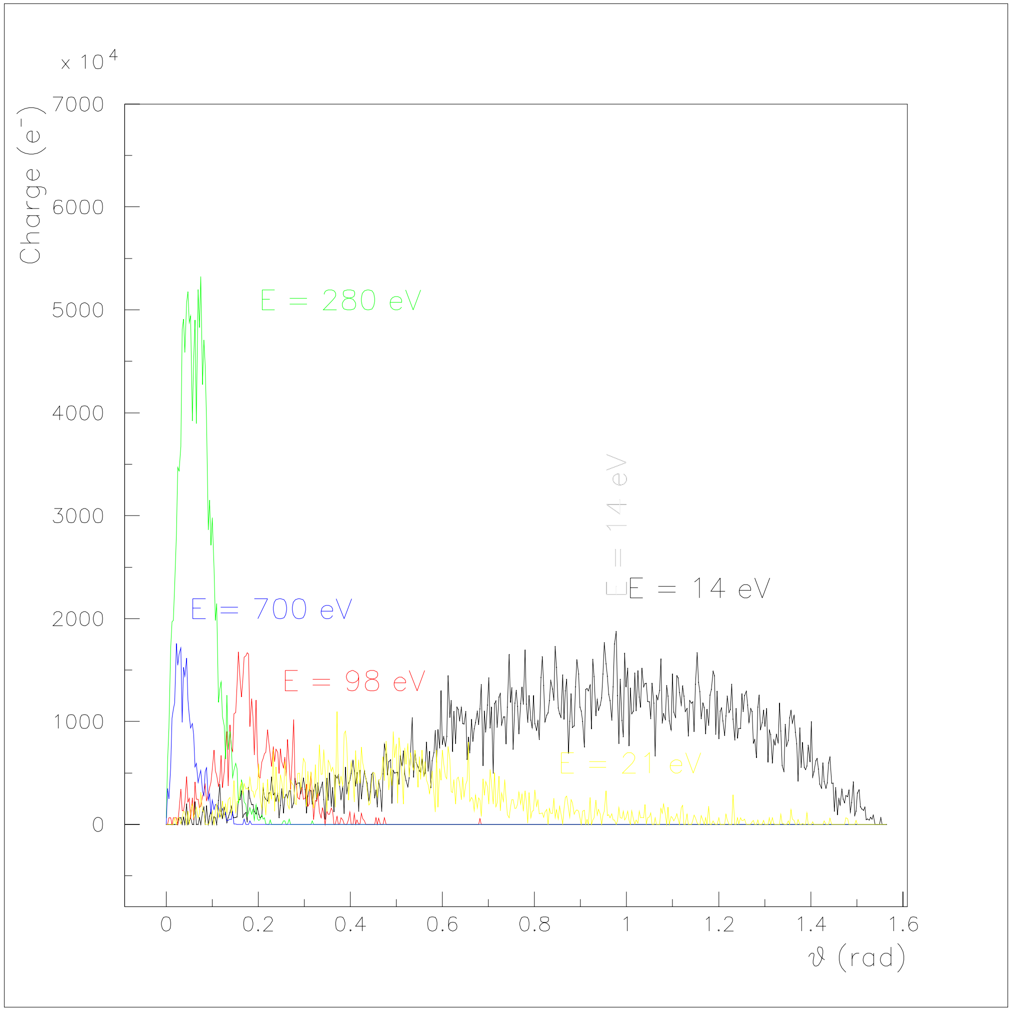

Angular distribution for different electron energies and LHC beam parameters [A. Arauzo, F.Z., 2000].

Single Bunch Effects

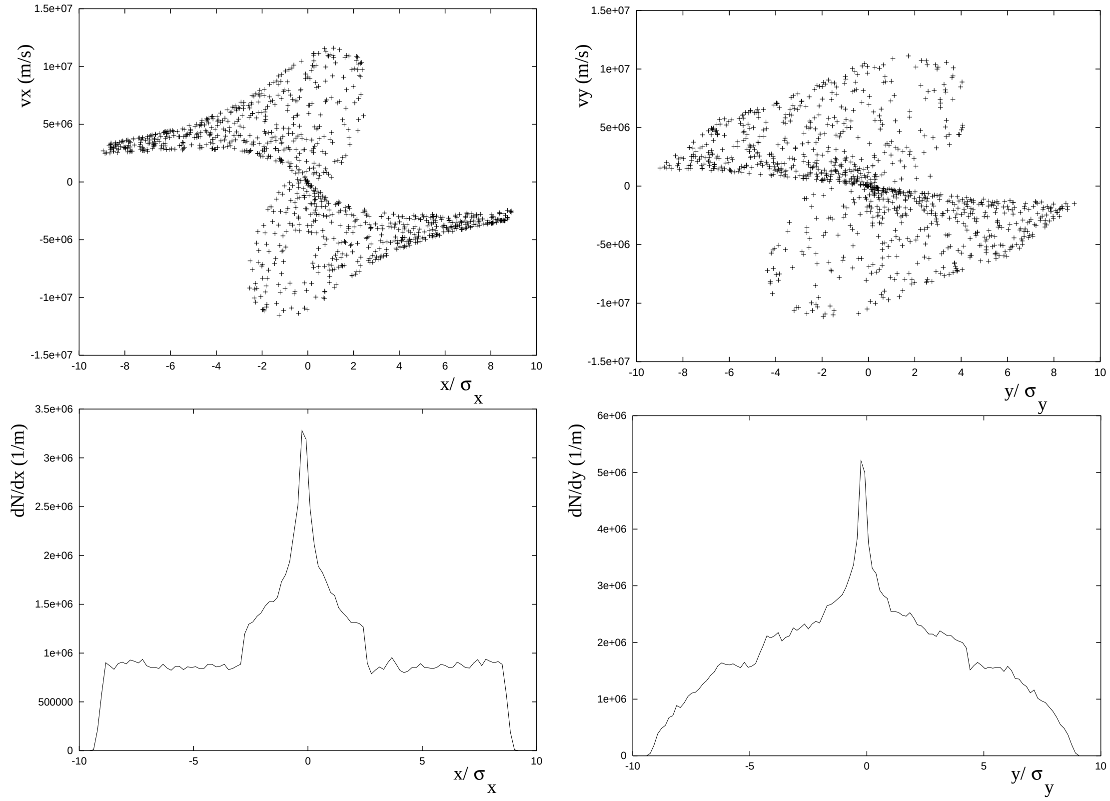

Snapshots of the horizontal and vertical electron phase space (top) and their projections onto the position axes (bottom). (G. Rumolo, 2001).

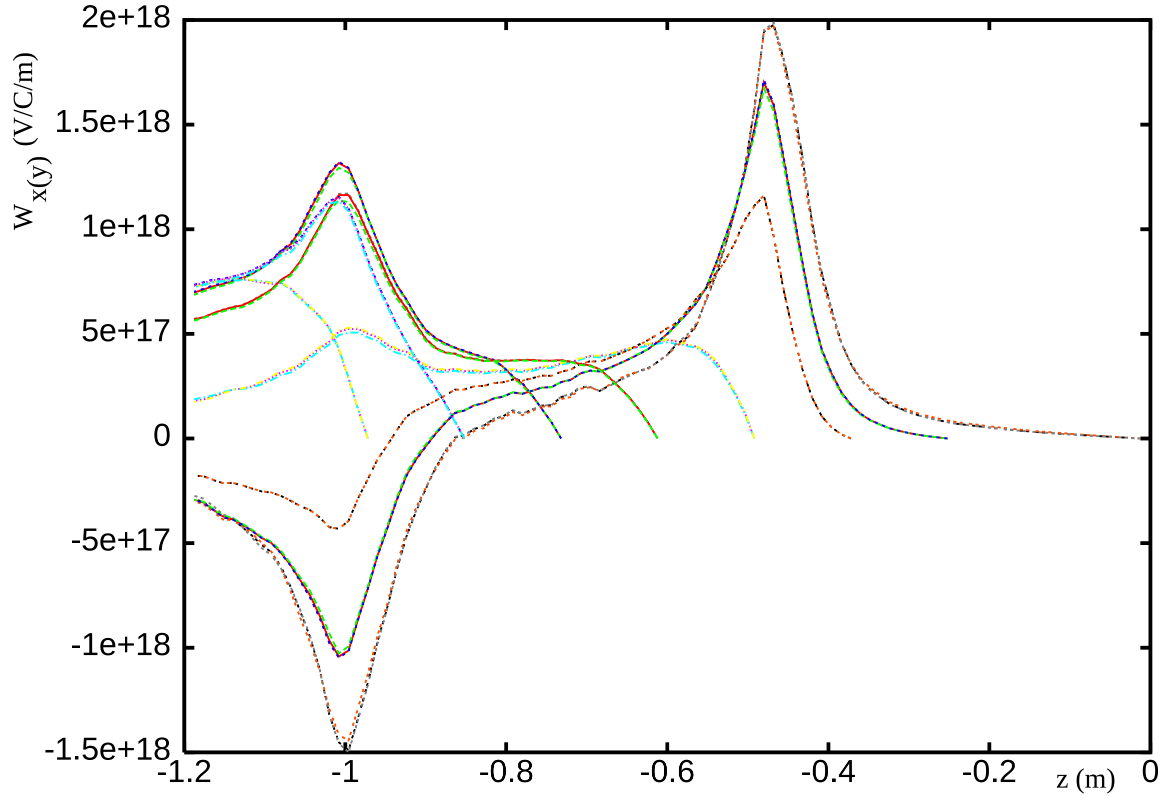

Simulated vertical wake field in V/m/C, excited by displacing vario
slices inside the Gaussian bunch, vs. position in m, for an SPS field-fr
region. The bunch center is at -0.6 m, the bunch head ($2\sigma_z$) on t
right. (G. Rumolo, 2001). Multiply by $4\pi/(Z_0 c) \approx 10^{-10}$ to get m

Ohmi fitted coasting-beam wake to resonator (ω_R, cR_S/Q, Q_R); then TMCI thresho
for $\omega_R \sigma_z / c \gg 1$: $N_{b,\rm thr} \approx 3\sqrt{\pi} Q_s Q_R \gamma (\omega_R \sigma_z / c)^2 / (cR_S/Q)/\beta_y/r_e$ (B. Zotter)

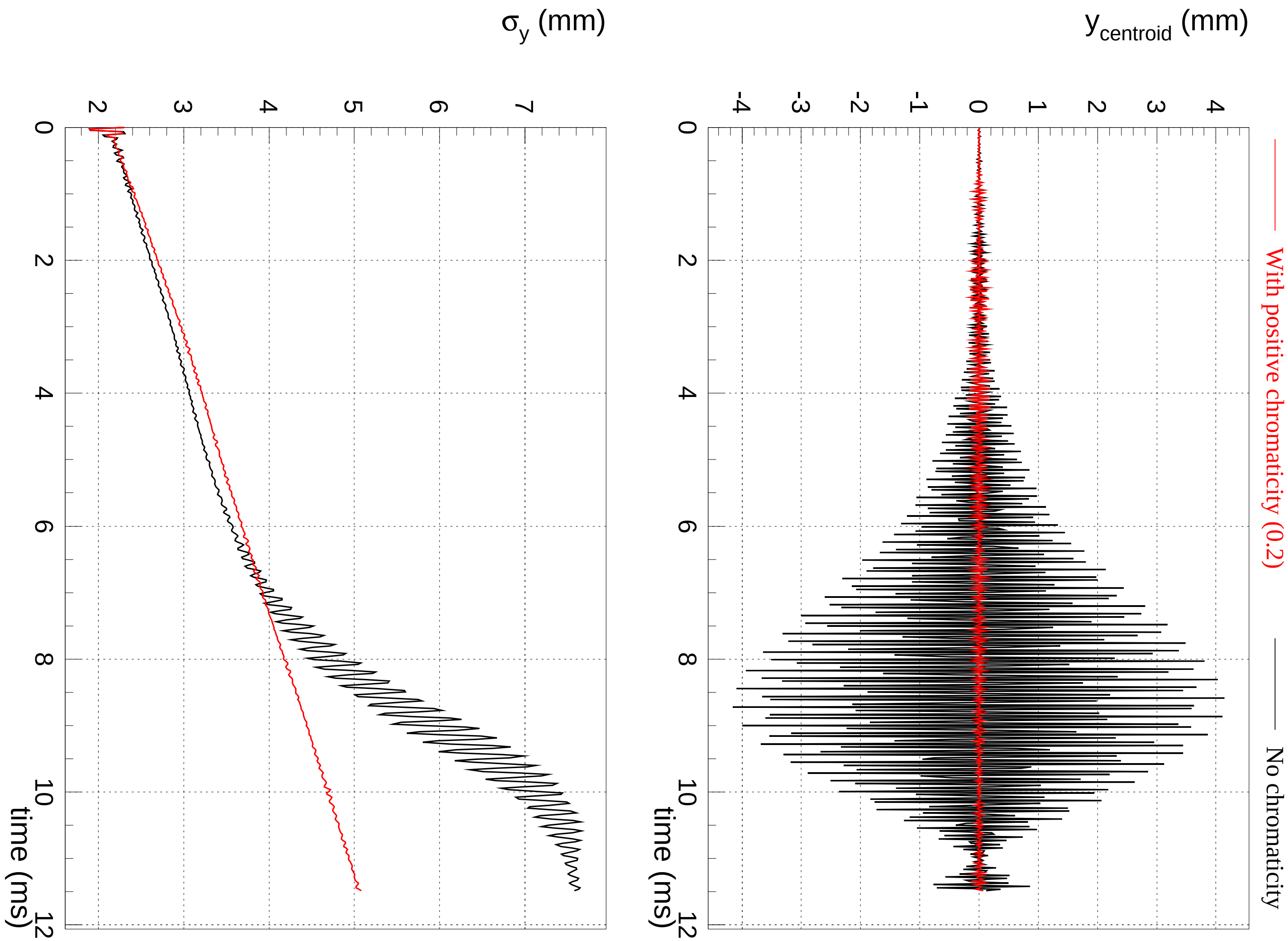

Simulated centroid motion and vertical beam size with zero and positive chromaticity in the SPS ($\xi_y = 0.2$). Machine broadband impedance is also included. (Courtesy G. Rumolo, 2001).

Role of Space Charge

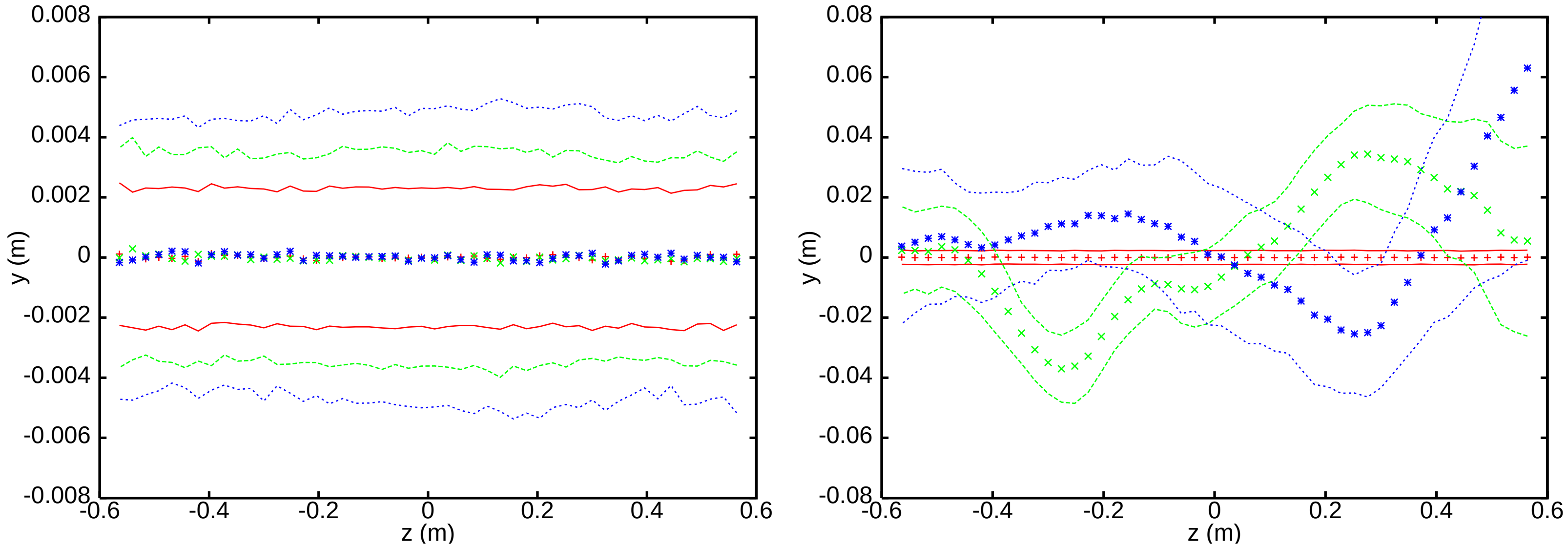

Simulated vertical bunch shape (centroid and rms beam size) after 0, 250, and 500 turns in the CERN SPS assuming an electron cloud density $\rho_e = 10^{12}$ m^{-3} without (left) and with (right) proton space charge at 26 GeV/c. (G. Rumolo, 2001).

4-Particle Model (inspired by K. Cornelis)

$z_1 = \hat{z}\cos\left(\frac{\omega_s s}{c}\right)$, $z_2 = \hat{z}\cos\left(\frac{\omega_s s}{c} + \frac{\pi}{2}\right)$, $z_3 = \hat{z}\cos\left(\frac{\omega_s s}{c} + \pi\right)$,
$z_4 = \hat{z}\cos\left(\frac{\omega_s s}{c} + \frac{3\pi}{2}\right)$ where $\hat{z} \approx \sigma_z$; $z > 0$: in front of center.

$$\omega_\beta(z) = \omega_{\beta,0}\left[1 - \left(\frac{\Delta\omega_\beta}{\omega_\beta}\right)_{\rm ec}\frac{z}{\sigma_z} - \left(\frac{\Delta\omega_\beta}{\omega_\beta}\right)_{\rm sc}\frac{z^2}{\sigma_z^2}\right]$$

$$\Delta\phi_i(s) = \frac{(\Delta\omega_\beta)_{ec}}{\omega_s}\sin\left(\frac{\omega_s s}{c} + \phi_{i,0}\right) + \frac{1}{2}\frac{(\Delta\omega_\beta)_{sc}}{\omega_s}\sin\left(\frac{2\omega_s s}{c} + 2\phi_{i,0}\right)$$

$$y_n = \tilde{y}_n \exp\left[-i\phi_i(s)\right],$$

$$\tilde{y}_n' = \frac{iNr_0W_0c}{8\gamma C\omega_\beta}\sum_{n', z_{n'} > z_n}\tilde{y}_{n'}\exp\left[-i\Delta\phi_{n'}(s) + i\Delta\phi_n(s)\right]$$

$$a \equiv \left(\frac{(\Delta\omega_\beta)_{ec} c}{\omega_s^2}\right) \frac{N r_0 W_0 c}{8\gamma C \omega_\beta}, \quad b \equiv \frac{1}{4}\left(\frac{(\Delta\omega_\beta)_{sc} c}{\omega_s^2}\right) \frac{N r_0 W_0 c}{8\gamma C \omega_\beta}$$

(1,4,2,3), (4,1,3,2), (4,3,1,2), (3,4,2,1), (3,2,4,1),(2,3,1,4), (2,1,3,4), (1,2,4,3).

$$\begin{pmatrix} \tilde{y}_1 \\ \tilde{y}_2 \\ \tilde{y}_3 \\ \tilde{y}_4 \end{pmatrix}_{T_s c/8} = \begin{pmatrix} 1 & 0 & 0 & 0 \\ (1-\sqrt{2})a + 2b & 1 & 0 & -\sqrt{2}a \\ (2-\sqrt{2})a & (a-2b) & 1 & (\sqrt{2}-1)a - 2b \\ a + 2b & 0 & 0 & 1 \end{pmatrix} \begin{pmatrix} \tilde{y}_1 \\ \tilde{y}_2 \\ \tilde{y}_3 \\ \tilde{y}_4 \end{pmatrix}_0 \equiv M_1 \begin{pmatrix} \tilde{y}_1 \\ \tilde{y}_2 \\ \tilde{y}_3 \\ \tilde{y}_4 \end{pmatrix}$$

$$\begin{pmatrix} \tilde{y}_1 \\ \tilde{y}_2 \\ \tilde{y}_3 \\ \tilde{y}_4 \end{pmatrix}_{T_s c/4} = \begin{pmatrix} 1 & 0 & 0 & -a - 2b \\ (\sqrt{2}-1)a + 2b & 1 & (2b-a) & (\sqrt{2}-2)a \\ \sqrt{2}a & 0 & 1 & (\sqrt{2}-1)a - 2b \\ 0 & 0 & 0 & 1 \end{pmatrix} \begin{pmatrix} \tilde{y}_1 \\ \tilde{y}_2 \\ \tilde{y}_3 \\ \tilde{y}_4 \end{pmatrix}_{\frac{T_s c}{8}} \equiv M_2 \begin{pmatrix} \tilde{y}_1 \\ \tilde{y}_2 \\ \tilde{y}_3 \\ \tilde{y}_4 \end{pmatrix}$$

$$P = \begin{pmatrix} 0 & 0 & 0 & 1 \\ 1 & 0 & 0 & 0 \\ 0 & 1 & 0 & 0 \\ 0 & 0 & 1 & 0 \end{pmatrix}$$

total matrix for one synchrotron period

$$M_{\rm tot} = (P M_2 M_1)^4$$

SPS: tune shift due to e^- cloud $\Delta Q_{\rm ec} \approx 0.03$, due to space charge $\Delta Q_{\rm sc} \approx 0.015$; constant wake $W_0 = 8\pi\rho_e C/N_b \rightarrow a \approx 19.7$ and $b \approx 2.5$.

Largest eigenvalue of matrix $M_{1/4}$ is 15.5 (300 μs rise time).

For $b \approx 20$ ($\Delta Q_{\rm sc} \approx 0.13$): 80 μs.

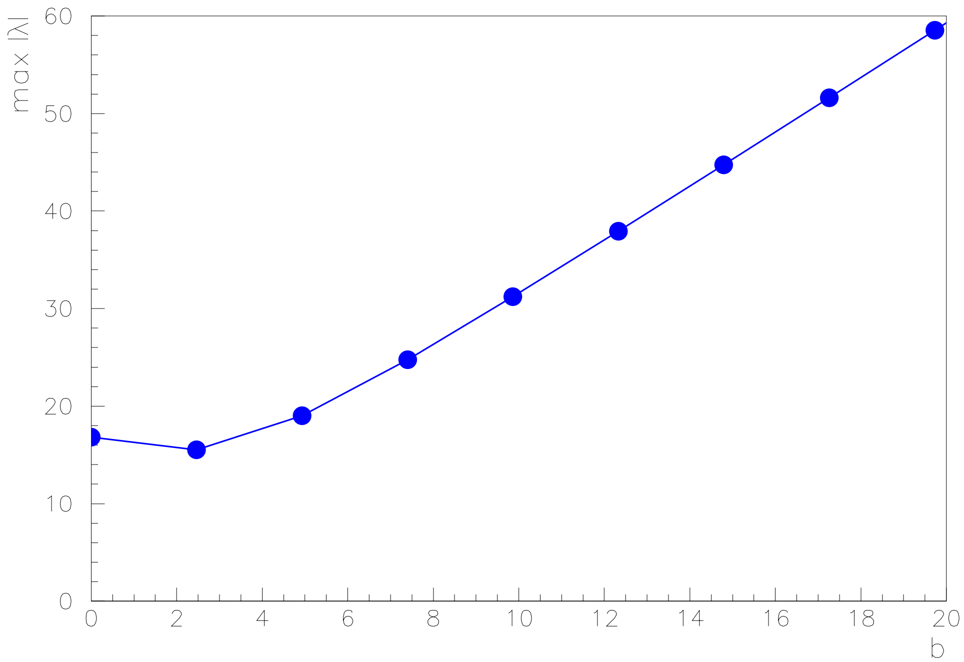

Maximum eigenvalue vs. space-charge parameter b.

Field-Free Region vs. Dipole Field

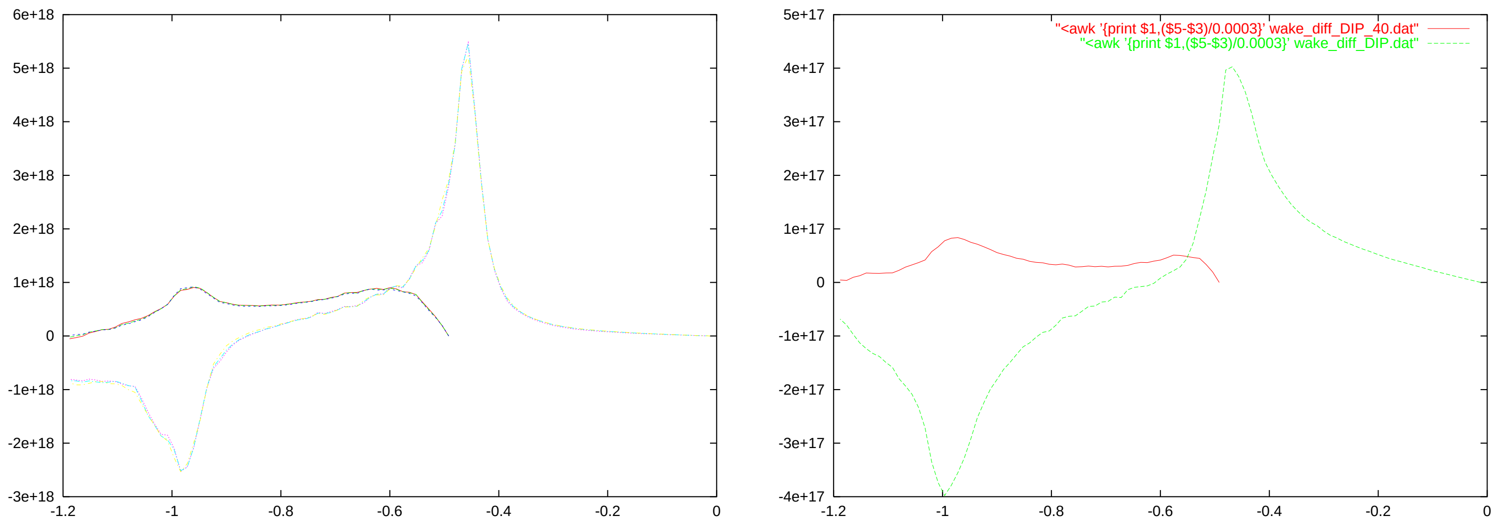

Simulated vertical wake field in V/m/C, excited by displacing the 1st and 41st slice inside the Gaussian bunch, vs. position in m, for an SPS field-free region (left) and dipole field (right). The bunch center is at -0.6 m, the bunch head ($2\sigma_z$) on the right. (G. Rumolo, 2001).

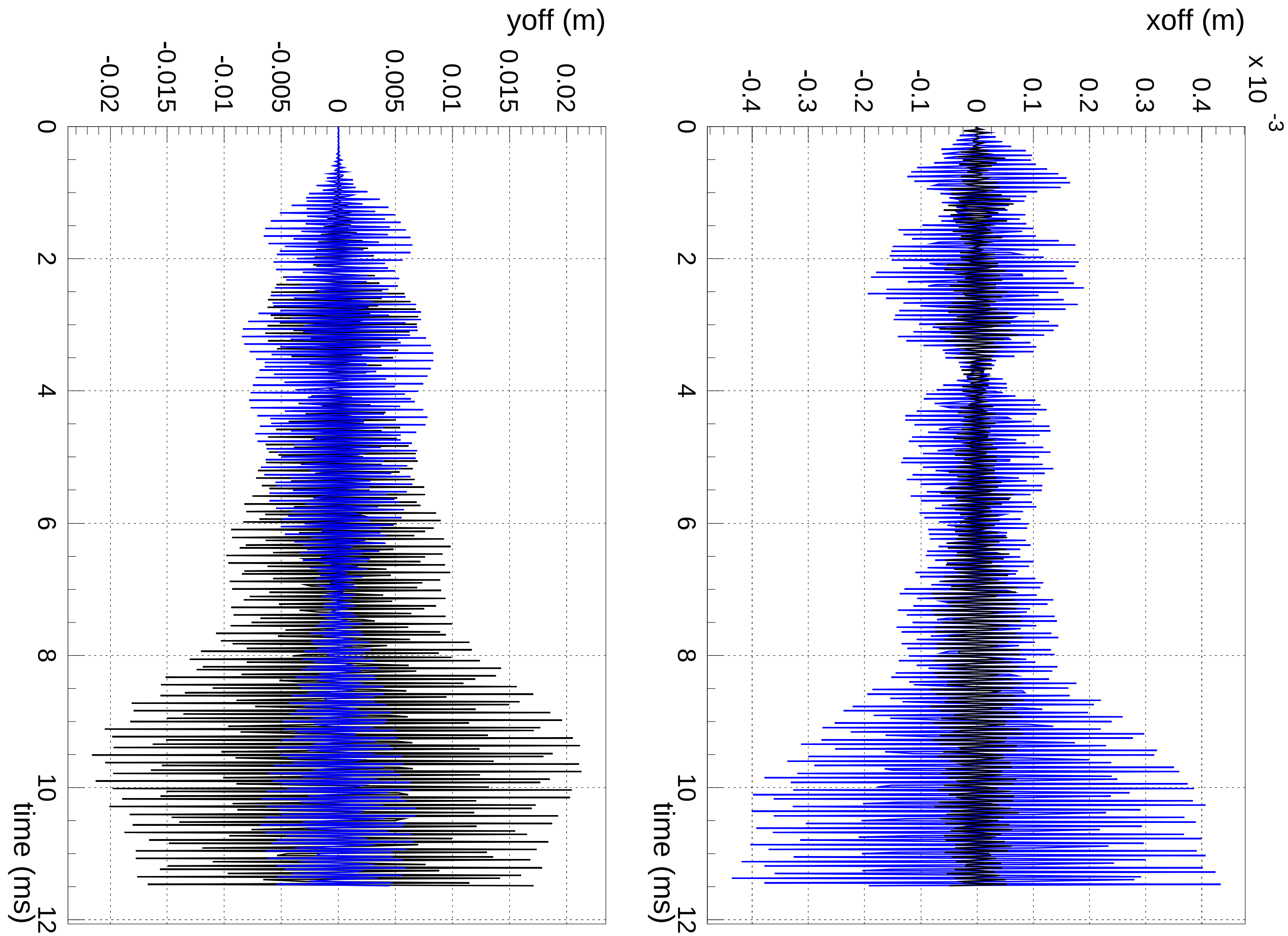

Simulated centroid motion in the SPS comparing a field-free region (blue) and a dipole field (black). Space charge is included. (G. Rumolo, 2001).

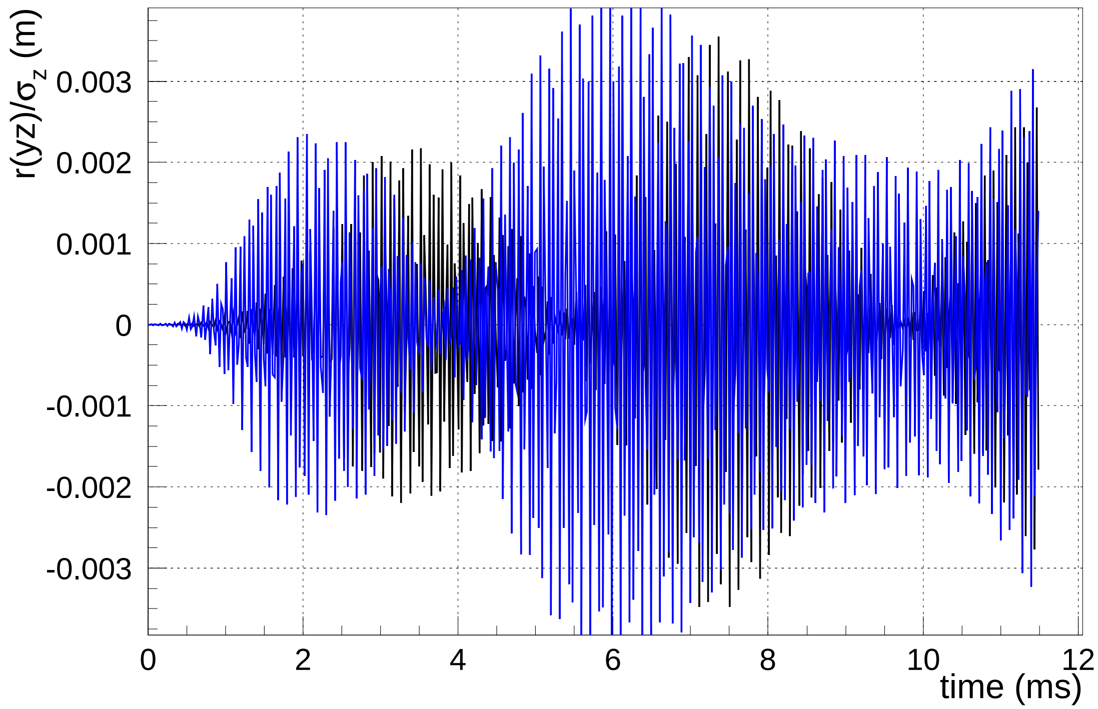

Simulated head-tail motion in the SPS comparing a field-free region (blue) and a dipole field (black). Space charge is included. (G. Rumolo, 2001).

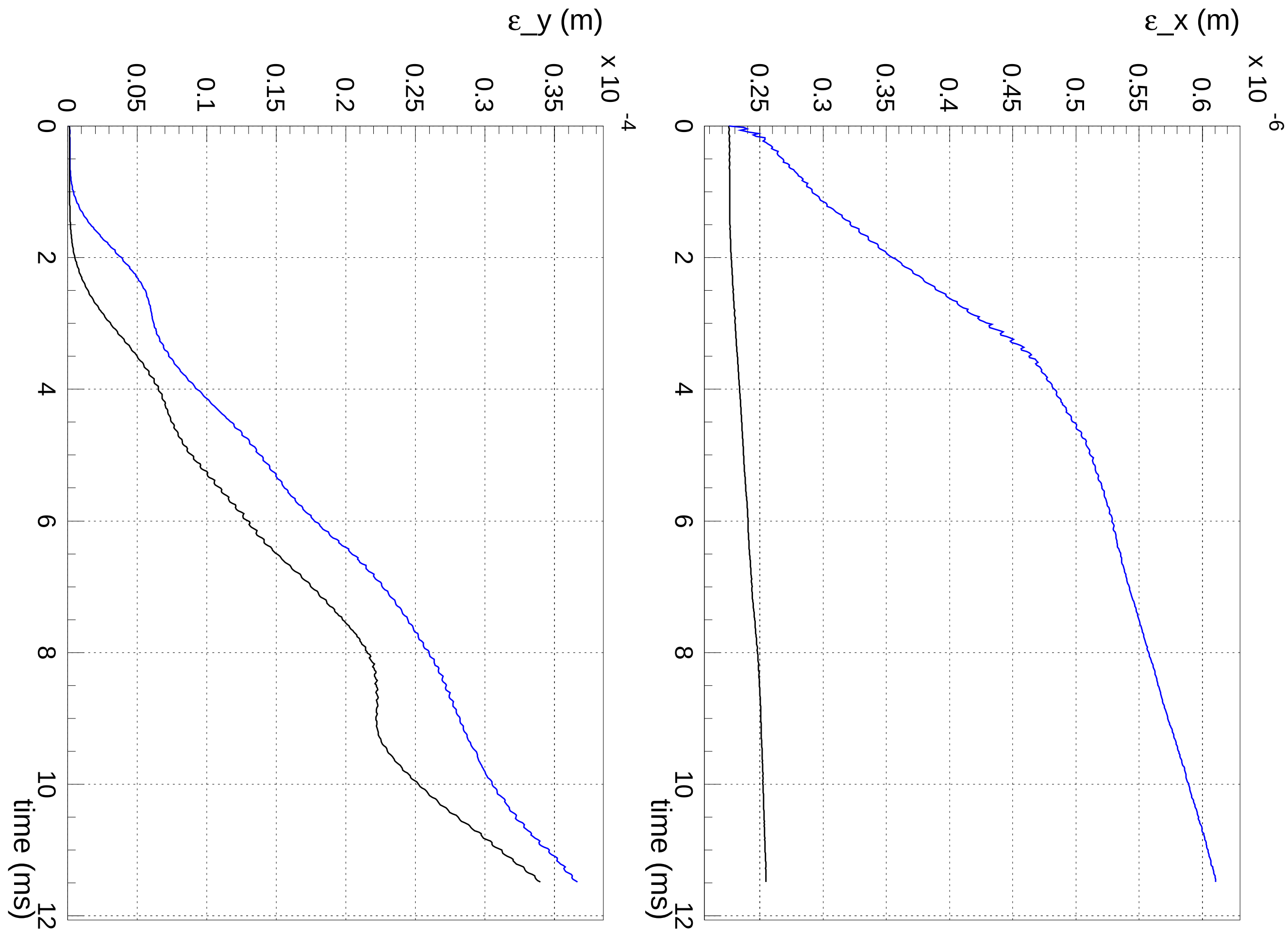

Simulated emittance growth in the SPS comparing a field-free region (blue) and a dipole field (black). Space charge is included. (G. Rumolo, 2001).

CERN

Electron Energies, Angles & Heat Load

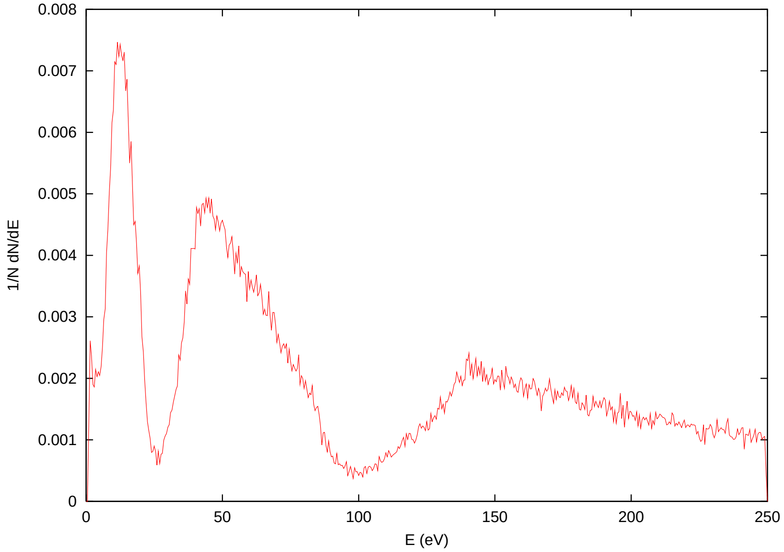

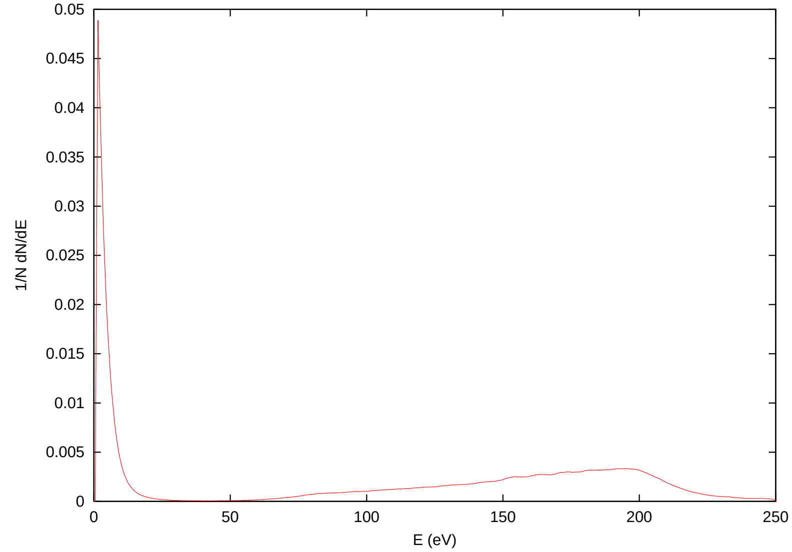

Energy distribution of e^-s incident on LHC chamber wall for a chamber radius $r = 158$ mm (left) and 29 mm (right) (G. Rumolo).

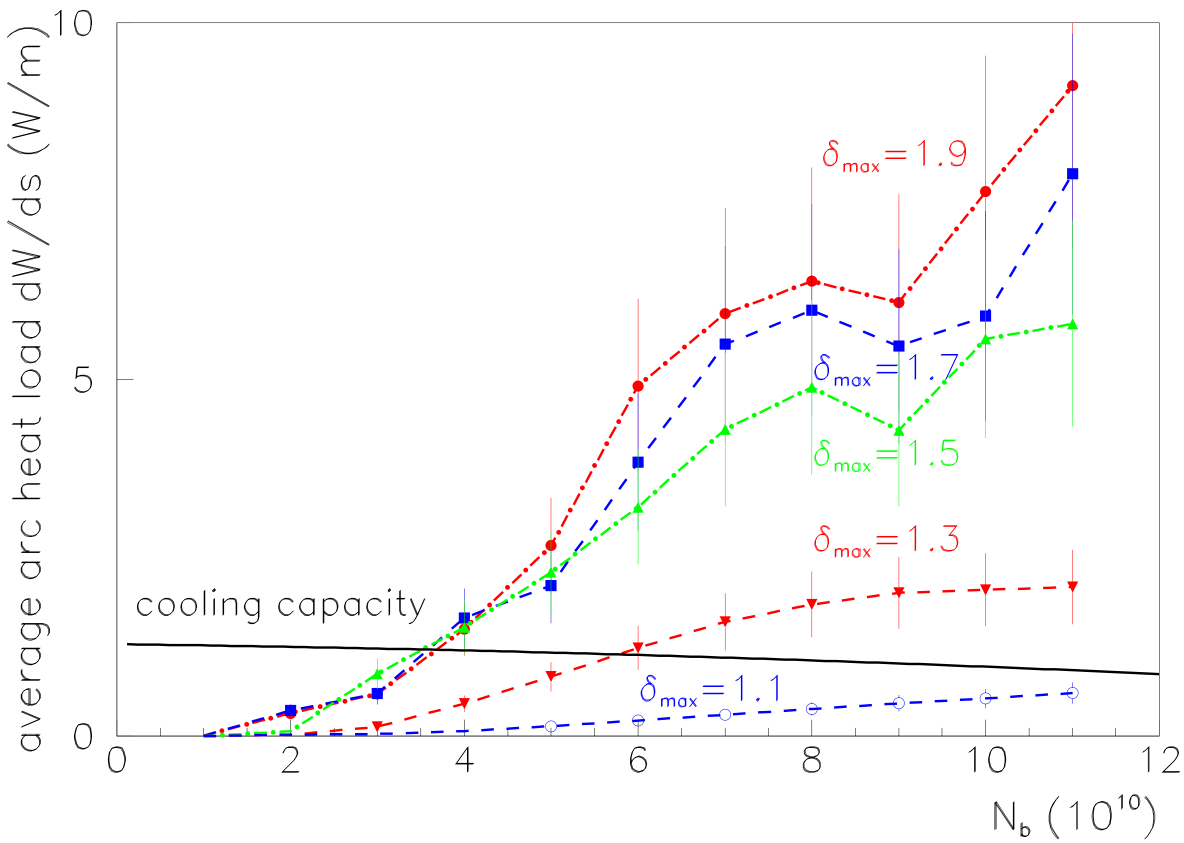

Average arc heat load and cooling capacity as a function of bunch population N_b, for various $\delta_{\rm max}$. Other parameters are $\epsilon_{\rm max} = 240$ eV, $R = 5\%$, $Y = 5\%$, and elastic electron reflection is included.

Electron Cloud Heat Load for Shorter Bunch Spacing (LHC Luminosity Upgrade)

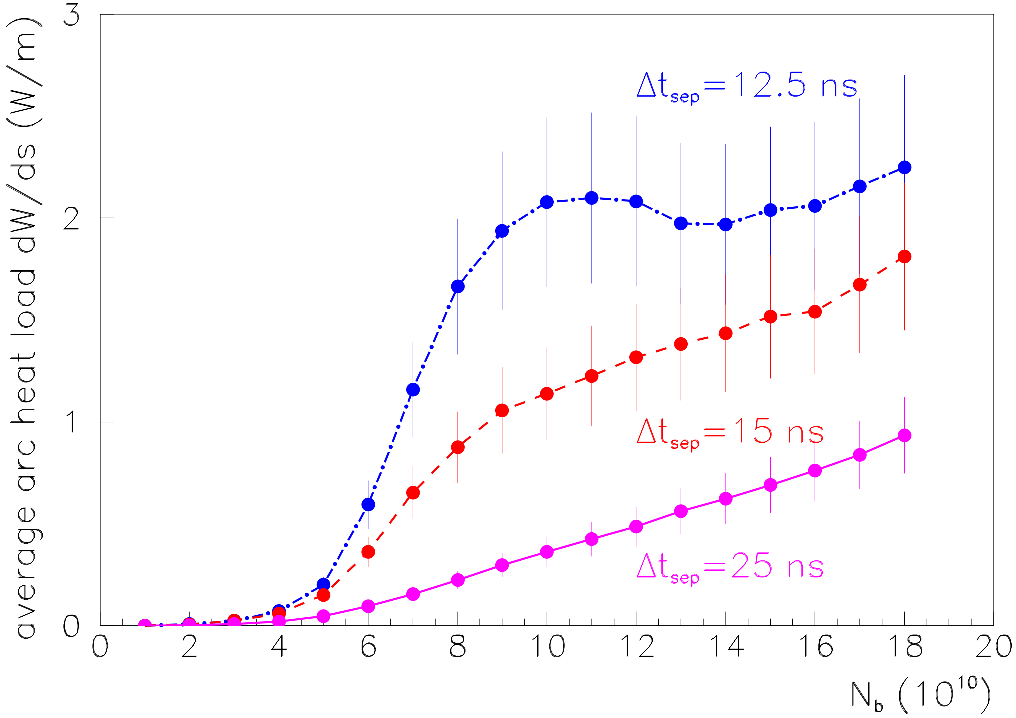

Average LHC arc heat load as a function of bunch population for bunch spacings of 12.5 ns, 15 ns, and 25 ns, and a maximum secondary emission yield $\delta_{\max} = 1.1$. Elastically reflected electrons are included.

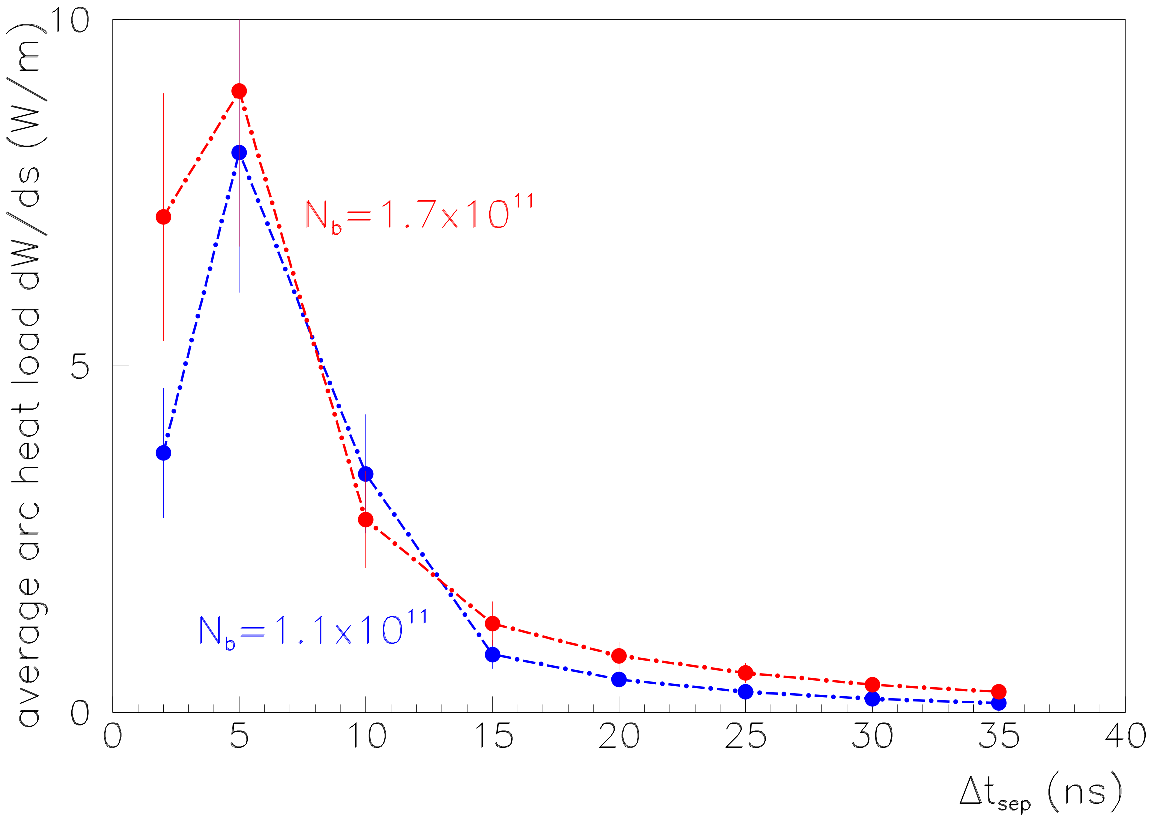

Average LHC arc heat load as a function of bunch spacing, for $\delta_{\rm max} = 1.1$ and various bunch populations.

LHCbeamscreen

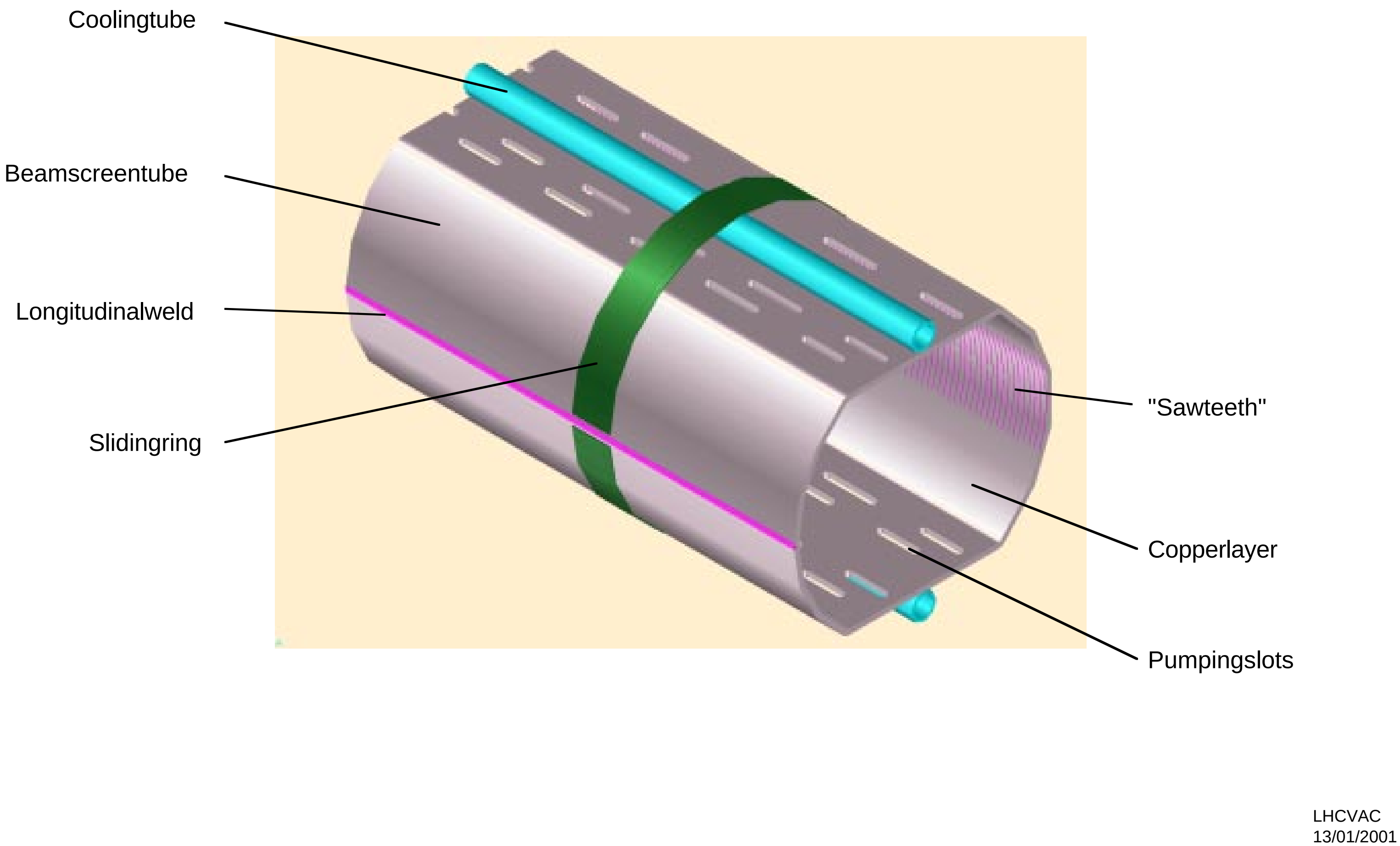

Schematic of LHC beam screen operating at $T \approx$5–20 K. (Ian Collins, 2001).

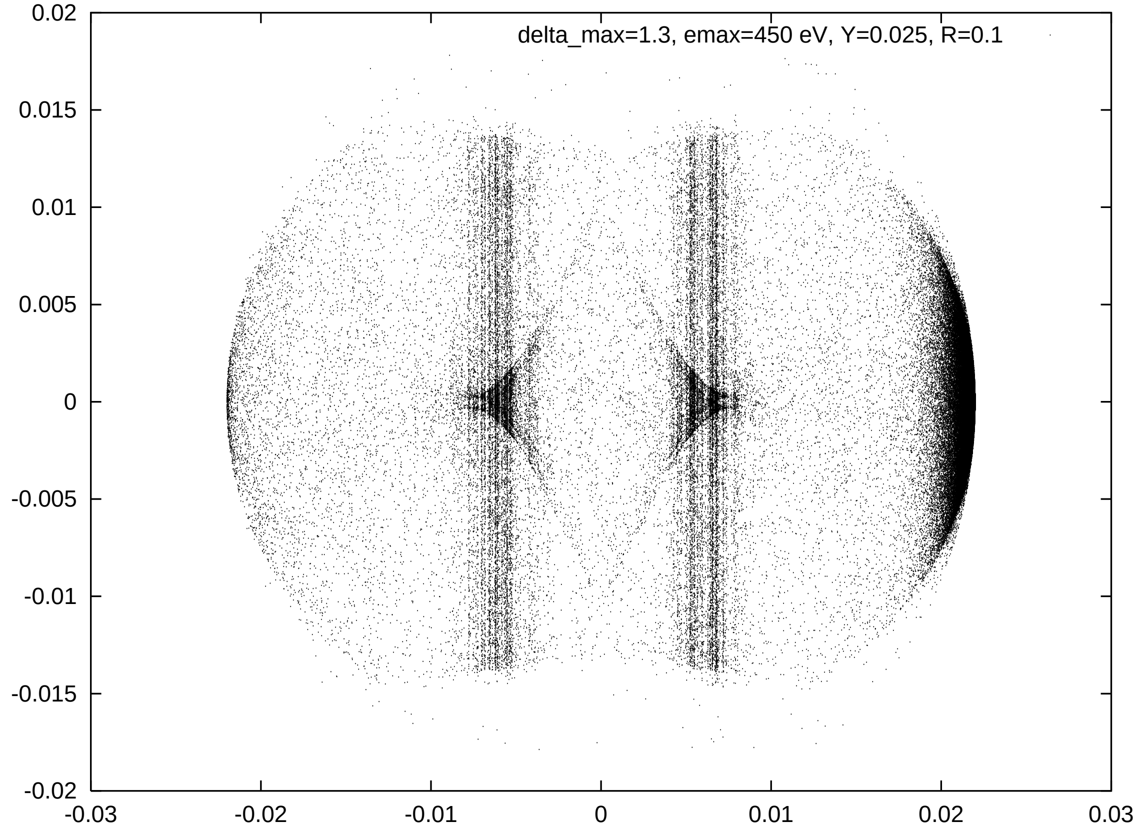

Snapshot of transverse e$^-$ distribution in an LHC dipole chamber (F.Z., 1997). Parameters: $\delta_{\rm max} = 1.3$, $\epsilon_{\rm max} = 450$ eV, $R = 0.1$, and $Y^* = 0.025$.

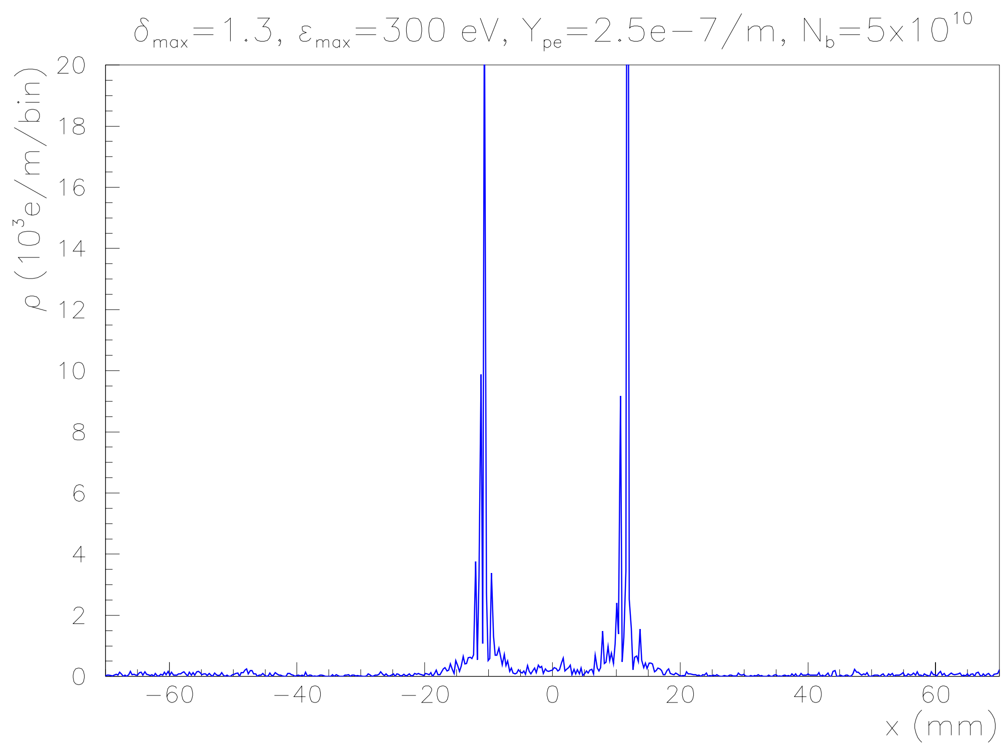

Projected horizontal electron charge density after 60 bunches in an SPS dipole chamber. Vertical peaks correspond to regions with large secondary emission. Parameters: $\delta_{\rm max} = 1.3$, $\epsilon_{\rm max} = 300$ eV, $R = 1$, pressure 50 nTorr, and 500 bins.

Conclusions

- simulated roughly build up consistent with observations for SPS, PS, KEKB, *e.g.*, build-up time, density, e^- on wall
- simulation results for single-bunch instability promising (effect of ξ, agreement with K. Ohmi's code).
- space charge strongly modifies the effect of e^- cloud (we may assume the same for beam-beam)
- dipole field changes the single-bunch wake field & instability
- e^- cloud could be *the* problem for linear colliders
- position of stripes reasonable, field-free regions $\longrightarrow$ further studies, *missing physics*?